Chapter 5

How to Study Smoking and Drinking with PET

Evan D. Morris, Molly V. Lucas and Kelly P. Cosgrove

Additional information is available at the end of the chapter

http://dx.doi.org/10.5772/57414

1. Introduction

1.1. Historical background

The era of imaging neuroreceptors in humans with PET was ushered in by Wagner et al. (1983) with a report in Science showing the first human brain scan of dopamine receptors (Wagner, 1983). The tracer was N-methylspiperone (NMSP) tagged with carbon-11. The brain that was scanned belonged to one of the authors. Ethical concerns notwithstanding, this act placed the researchers in the good company of famous scientists throughout history who had experimented on themselves. The publication of this paper excited the field and garnered some publicity as well (see Figure 1). Although the study did not employ the quantitative analysis techniques we describe below, it presaged some of the key concepts. Namely: (1) early images contain mostly blood flow information; (2) late images primarily reflect binding; (3) radioactive tracer in the target tissue can be "free" or "bound", which often necessitates the examination of a "reference region", which is devoid of receptor sites; (4) co-injection of radiolabelled tracer with an *excess* of unlabeled tracer can be used to prevent radiotracer from binding and thus measure unbound (aka, non-displaceable) signal by itself. Injection of excess unlabeled tracer is generally not performed in humans; in this case, it was done in baboons. As we discuss below, the ability to use PET to measure receptor number or some index thereof opens up additional measurement possibilities which take advantage of a key concept: competition. In the Wagner paper, the competition was between hot (labeled) and cold (unlabeled) tracer (Wagner, 1983). In another ground-breaking paper that followed it, the competition was between a radiotracer and an unlabeled neuroleptic drug (Farde et al., 1986). Farde and colleagues did what amounts to the first drug occupancy study with PET using the tracer, [^{11}C]raclopride, in 1986. Their paper was intended to examine the occupancy level of drugs for schizophrenia in treated schizophrenics by examining the degree of tracer blocking at the dopamine D2 receptor sites achieved by each patient's respective drug. Whereas Wagner et

al. could examine the difference between a baboon at baseline and following a co-injection of tracer with an excess of cold NMSP (Wagner, 1983), Farde et al. did not ask their patients to go off medication to get a baseline measurement of tracer binding (Farde et al., 1986). So how did they make an assessment of drug occupancy, which requires at least two measurements? They extrapolated what baseline binding might have been in their schizophrenics from a cohort of control subjects. Provocatively, they found that three schizophrenics undergoing (successful) treatment with different drugs all had receptor occupancies of very similar levels. Their approach would likely not pass muster today, but at the time, the paper was highly innovative, and it foreshadowed one of the major usages of PET and neuroreceptor tracers: measuring target occupancy by drugs in people.

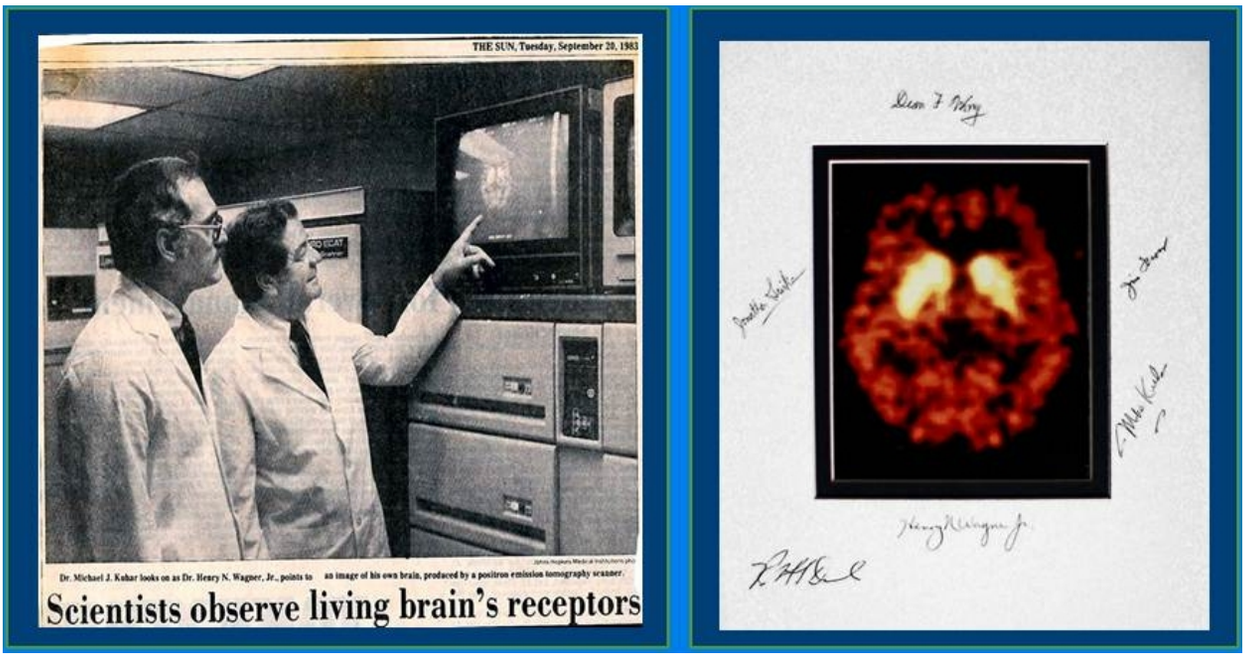

Figure 1. Left) Newspaper clipping from the Baltimore Sun, Sept 20, 1983, shows senior authors, Drs. Henry Wagner, Jr. and Mike Kuhar observing the first images of D2 receptors in a human brain, *in vivo*. (Right) A keepsake from the experiment adorns the offices of many of the landmark study's participants. Signatures, from the center bottom going clockwise, Wagner, Robert Dannals, Joanthan Links, Dean F. Wong, Jim Frost, and Kuhar. Photos care of M. Kuhar.

1.2. Basics

1.2.1. Molecular specificity

PET is unique among medical imaging modalities for its exquisite molecular specificity. From this specificity, PET derives its unique ability to image highly selective biological *processes* – that is, to act as a *functional* imaging modality. In the brain (and everywhere in the body), different processes are facilitated by highly specialized molecules. Individual enzyme molecules exist to catalyze highly selective and uni-purpose biochemical reactions. Unique receptors and transporters exist to bind highly specialized endogenous ligands and carry out unique physiological functions. Some of the functions of interest that are controlled by

http://dx.doi.org/10.5772/57414

individual molecules and which we may want to image are shown in Figure 2. PET can image any of these molecular targets provided two obstacles have been overcome. First, a tracer molecule that binds or interacts with the target site must exist and be labeled with a positron emitting isotope (typically, carbon-11 or fluorine-18). Second, it must be possible to deliver the tracer to the target site. In brain imaging, the most likely cause of tracer failure is the inability of the tracer to cross the blood brain barrier to access the target.

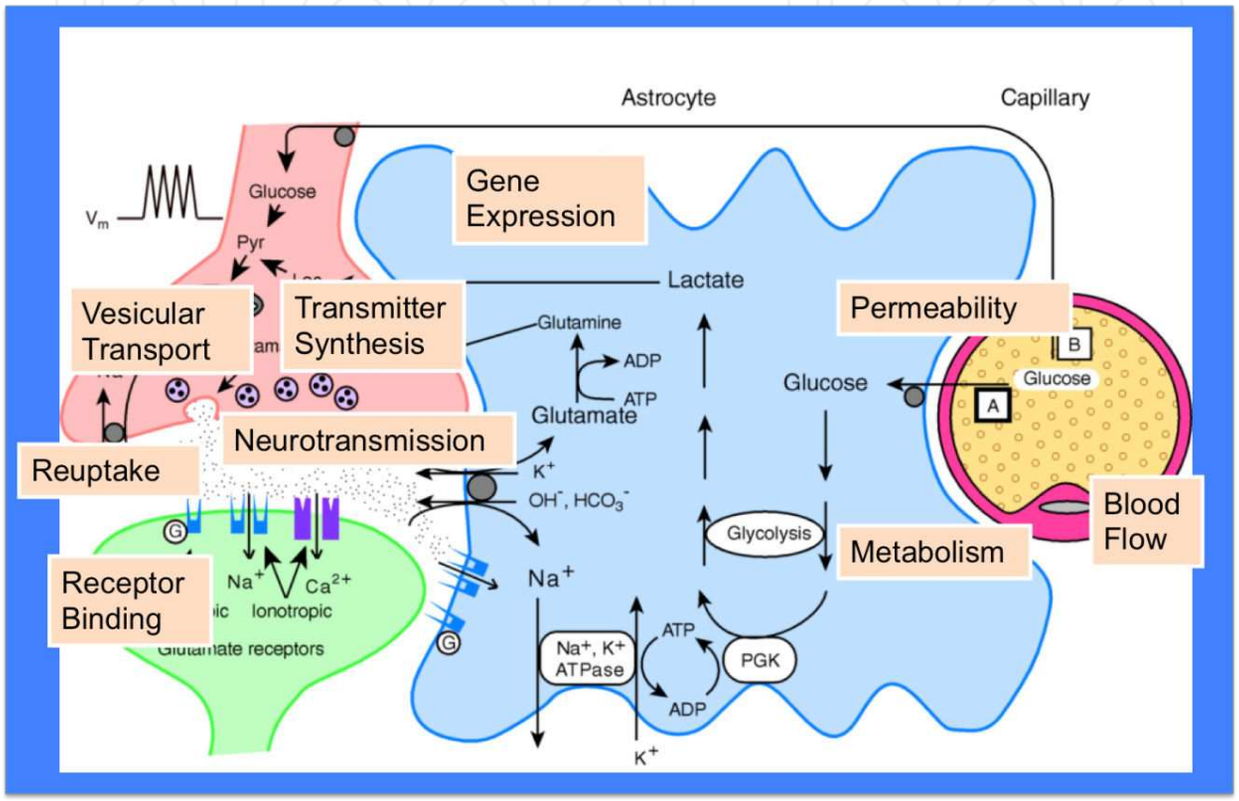

Figure 2. Molecular processes that can be imaged with the appropriate PET ligand. Figure modified (Pellerin et al., 1994).

1.2.2. Many tracers for many targets

At this writing, there are tracers for many of the common neurotransmitter receptor sites: dopamine (D_2/D_3 and D_1), serotonin ($5HT_{1a}$, $5HT_{1b}$, $5HT_4$…), and transporter sites (DAT, SERT, NET…). Tracers generally arise through one of three pathways. (1) Radiolabeling of a dye or other molecule that is known to be selective for a particular target of interest (e.g., [^{11}C]PIB arose from the radiolabelling of thioflavin-T) (Mathis et al., 2002). (2) Radiolabeling of a candidate drug for the target molecule of interest. Such candidate compounds may have been failed drugs (adverse drug side-effects on patients, kinetics too rapid to sustain clinically useful levels in blood and tissue) but make good tracers (no adverse side-effects, because tracers are given in micro-dose amounts, favorably rapid kinetics). (3) De novo design of new PET tracer based on knowledge of the structure of the target molecule.

1.2.3. Specific binding vs. nonspecific background

Tracers are administered to subjects intravenously and travel to the brain via the circulation. Once they traverse the blood brain barrier (typically by passive diffusion), they can follow three possible fates. Some tracer molecules remain free (unbound), eventually clear back to the vasculature and are removed from the organ. Other tracer molecules, once inside the tissue, may bind to the specific target of interest. Because no tracers are perfectly ideal in their behavior, some molecules are bound nonspecifically (nondisplaceably) before clearing from the tissue. Thus, in toto, radioactive emissions that are detected by the PET scanner are a (time-varying) sum of emissions of radio-isotopes on tracer molecules in all four different possible states: blood-borne, free in tissue, specifically bound to a receptor or other target molecule, or nonspecifically bound (Figure 3). The PET scanner records all of these emissions indiscriminately. Nothing about the photons that are emitted from an annihilation event in the blood or tissue makes their original state knowable from the detected signal. Thus, on any given *static* PET image (a single image summed over a time frame), the desired signal – i.e., the amount of specifically bound tracer – cannot be discerned easily because the signal is confounded by background activity coming from tracer in its three other possible states.

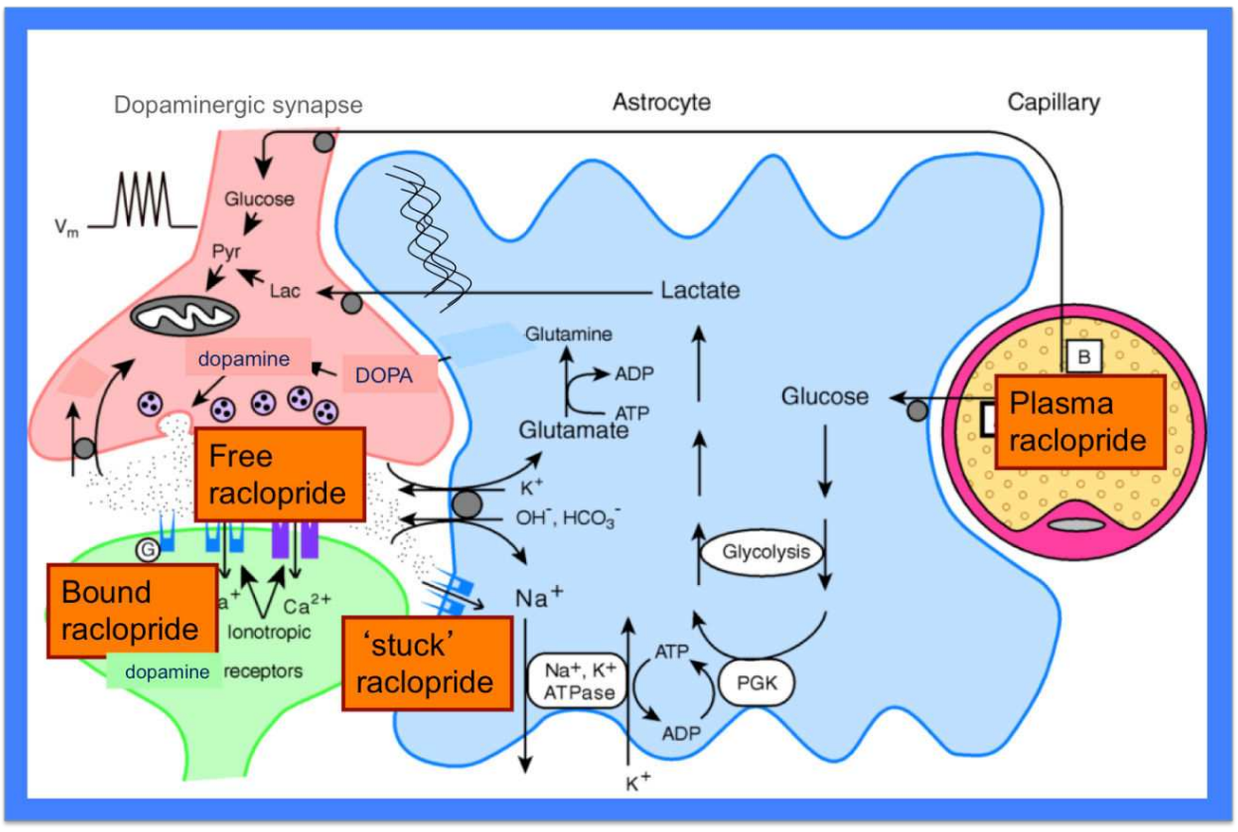

Figure 3. Possible states of an injected radiotracer. The states can be thought of as distinct, interconnected pools. Figure modified (Pellerin et al., 1994).

The one thing that allows us to differentiate the binding from the background is the difference in temporal behavior of the various tracer states. The persistence of activity (in a sense, the

http://dx.doi.org/10.5772/57414

residence time) in each of the plasma, free, bound, and nonspecific pools is different (see curves in Figure 4). Thus, to identify the specific binding component of the total PET signal (green curve on Fig. 4, also called a time-activity curve (TAC)), we must (a) acquire dynamic data (over many time frames), (b) identify an input function to the system (either plasma radioactivity or image-derived), and (c) apply a mathematical model to separate the dynamic data into its constituent parts.

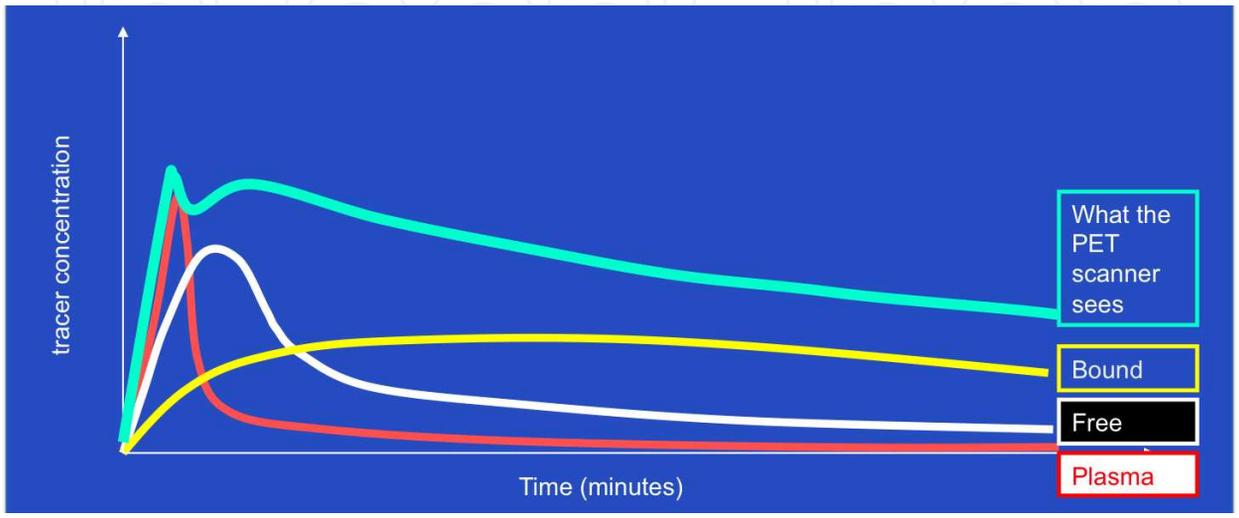

Figure 4. Different pools (compartments) of tracer activity are distinguishable by their different kinetics. Plasma activity (red) is cleared fastest. The free tracer pool (white) is slightly slower. The bound tracer pool (yellow) persists for longest. The PET scanner measures the sum of all the radiactivity (green).

1.2.4. Binding potential as endpoint

The most common endpoint for imaging neuroreceptor or neurotransmitter targets with PET is the compound parameter, binding potential (BP). The term was first introduced by Mintun and is equivalent to the steady state ratio in the target tissue of specifically bound tracer to free tracer (Mintun et al., 1984). Binding potential is a "compound" parameter, because it is equivalent to the ratio of individual rate constants (specifically, the association and dissociation rate constants). The rate constants arise in the standard compartmental model used to describe a TAC measured in a region of interest in the dynamic PET images. Readers should be aware that there are a few variations on the definition of binding potential (Innis et al., 2007). The definitions differ by what data are used as the input function to drive the particular kinetic model and by what assumptions are made. Nevertheless, the general principle can be stated: BP can be estimated as the steady state ratio of bound to free tracer. BP is also proportional to the available binding sites and inversely proportional to the equilibrium dissociation constant, K_D, of the tracer for the binding site. The former concept is diagrammed in Figure 5. We see that there are four species of interest in imaging neuroreceptor targets. First, the receptor, second, the tracer molecule that binds to the target and emits a positron, third, the unlabeled tracer which also binds to the target but emits no positron, and fourth, the endogenous ligand that is also specific for the target but (naturally) emits no positron.

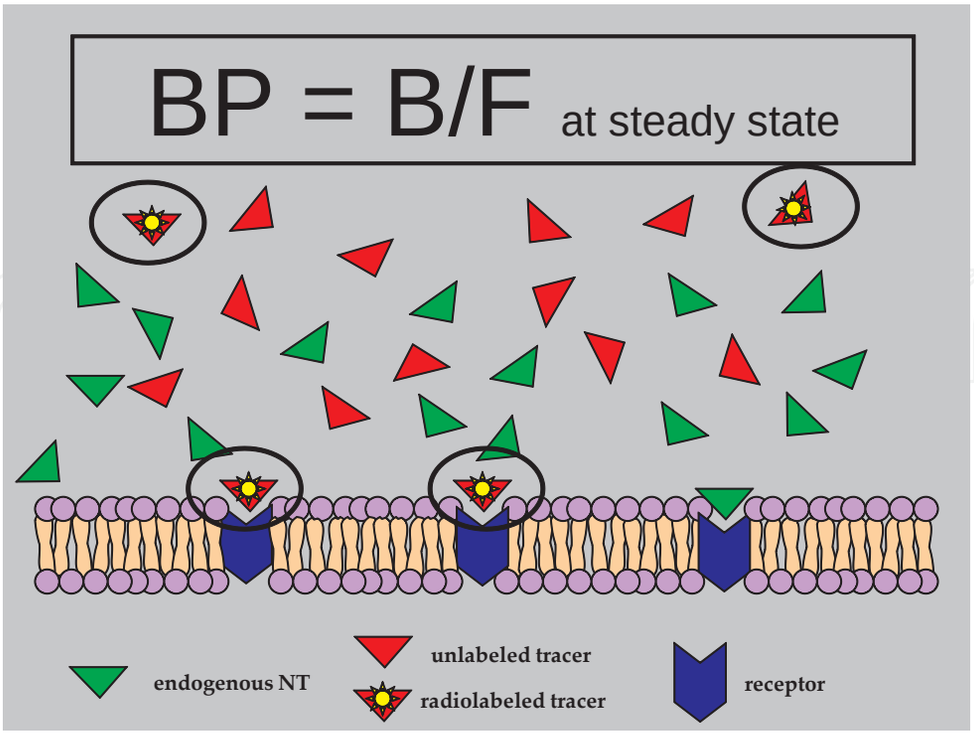

Figure 5. Binding potential depicted as bound over free tracer (red with star) at steady state. Receptor (or transporter) molecules (blue) may be embedded in a cell membrane. Two other species compete with tracer for limited binding sites: cold tracer (red), endogenous ligand (green).

1.2.5. Changes in receptor number

As previously stated, BP is proportional to number of available receptor binding sites and typically serves as a convenient surrogate for receptor density, provided the proportionality constant can be taken as a constant across the groups or conditions being compared. When BP is estimated from dynamic data using the arterial plasma concentration of tracer as the input function, the proportionality between BP and Bmax is simply $1/K_D$. (i.e., $BP = B_{max}/K_D$). Perhaps the most common use of BP as an endpoint is to assay receptor density (e.g., dopamine D_2R) in two groups of subjects (e.g., healthy controls and cocaine addicts) and compare them (Martinez et al., 2003; Volkow et al., 1997). In such a case, the density of receptors may be believed to have a direct functional role in a disease process. Alternatively, receptor number can be a surrogate marker for number of functioning neurons. Consider Parkinson's disease (PD), which involves loss of nigro-striatal connections. Because functioning nigro-striatal projections contain D2 receptors and dopamine transporters on their striatal terminals, absence of such sites in a PET scan is indicative of disease progression and attendant loss of neurons. Low dopamine receptors and low dopamine transporters have each been demonstrated with either [^{11}C]raclopride or [^{11}C]CFT, respectively, by comparing the BP for healthy controls to that of PD patients (Biju et al., 2009; Brooks et al., 1990). The schematic in Figure 6 represents the case of low BP caused by low receptors (Figure 6 should not be interpreted too literally. e.g., in the case of PD, the entire cell membrane along with the receptors might be missing).

http://dx.doi.org/10.5772/57414

1.2.6. Changes in endogenous neurotransmitter

Another popular use of BP is as a measure of steady state neurotransmitter level. Such measurements are typically made by comparing BP in the same subject at baseline and in a drug or treatment condition. This can be done via two paired bolus injections of tracer or via one bolus plus infusion of tracer (see section 1.2.10 below). Typically, a drug will be given prior to the PET scan. The drug (e.g., cocaine, methylphenidate, amphetamine) will cause elevation of endogenous neurotransmitter, which will in turn occupy more binding sites. As a result, fewer binding sites will remain available for binding by the labeled tracer, and the measured BP will be lower than at baseline. The fractional change in BP is the parameter that is most often reported as an indicator that there has been a prolonged change in neurotransmitter level (Here, "prolonged" simply means on the order of, or longer than, the scan duration). Figure 7 illustrates the principle using the same scheme as in Figures 5 and 6. Because specific binding sites exist in limited number, the approach to full binding will follow a saturation curve. That is, for greater and greater amounts of neurotransmitter release, we expect to see less and less incremental reduction of binding potential.

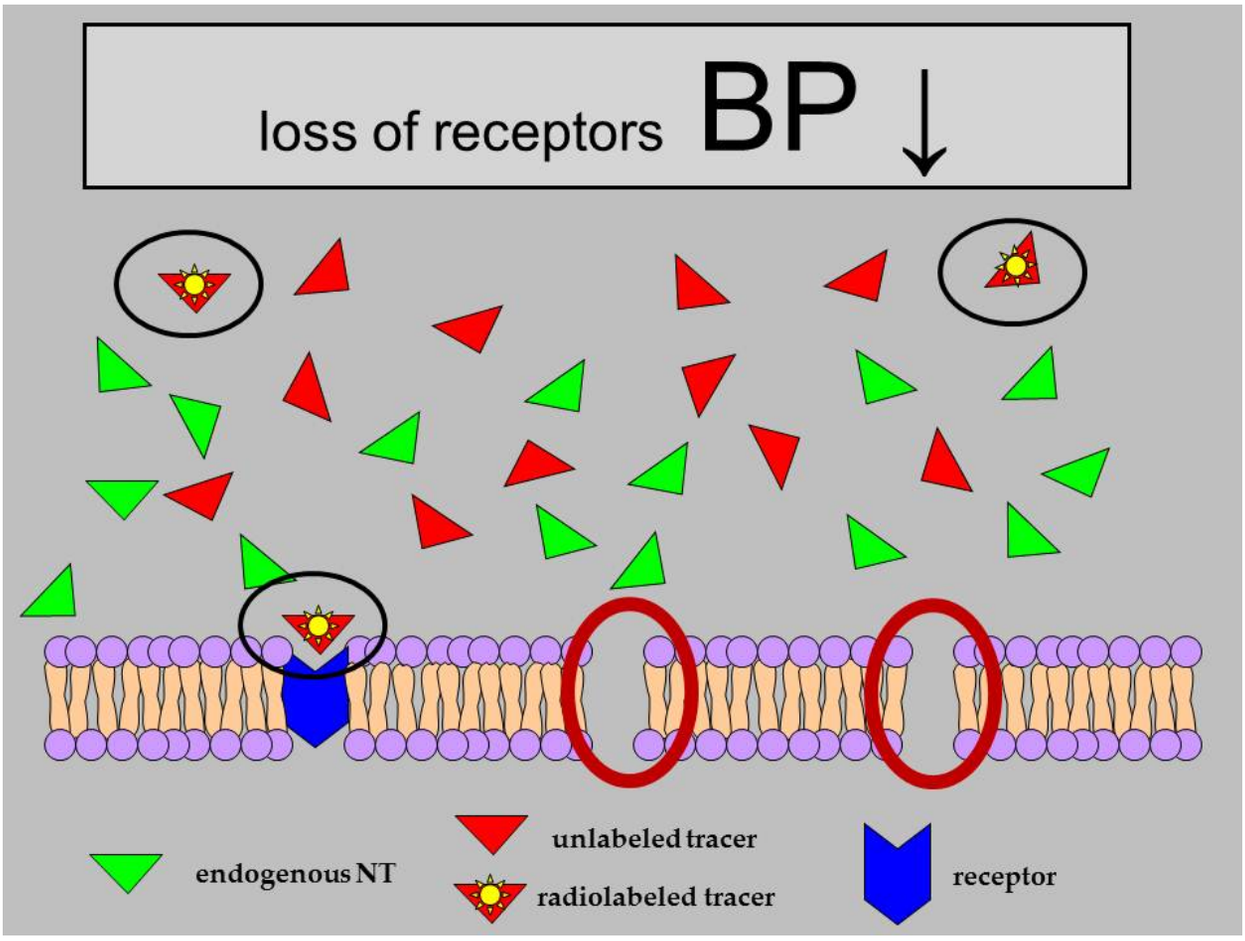

Figure 6. Lower Binding Potential reflects lower receptor density. (Compare to Figure 5).

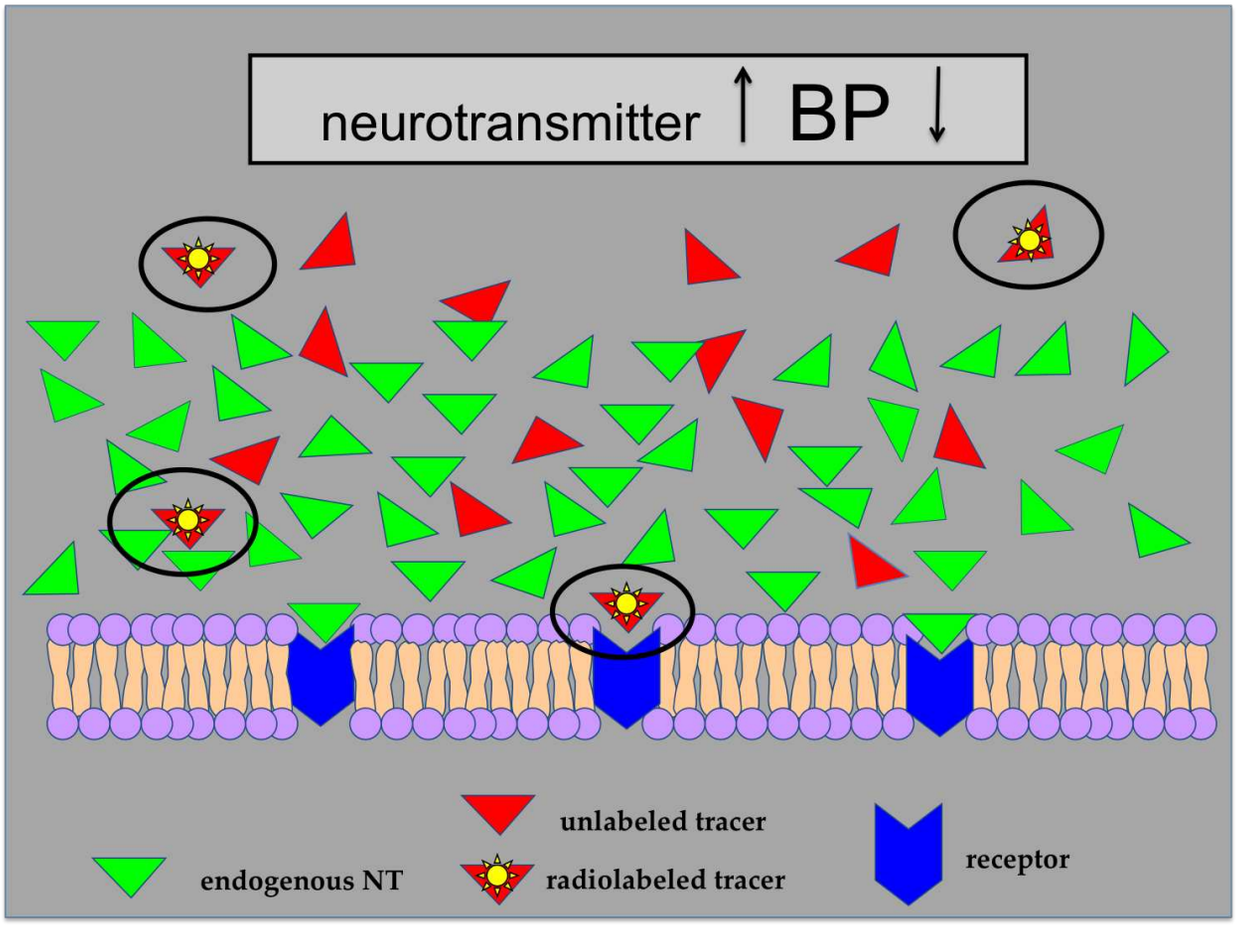

Figure 7. Elevation of endogenous neurotransmitter (green triangles) blocks available receptors and is detected as a reduction in BP.

1.2.7. Changes in occupancy by an exogenous drug

A third common usage of PET and BP is for measuring occupancy of receptor sites by exogenous (unlabeled) drugs. This is a popular use of PET by pharmaceutical companies who typical want to know three things: (a) does their candidate drug get into the brain, (b) does the candidate drug hit the intended target, and (c) what is the relationship between dose of the drug and percentage occupancy of the available (target) receptors? When companies are ready for a drug-occupancy study with PET they usually already know the safe dose range of the drug (i.e., the range of doses that cause little to no adverse side-effects). They also have a desired occupancy level in mind that will produce the desired drug effects. The question that PET can answer is: what is the receptor occupancy for each dose level in the allowable range. This relationship is characterized by an ED_{50} (drug dose at which 50% occupancy is achieved) and an E_{max} (maximal achievable level of binding if there were no upper limit on dose). Just as with elevation of endogenous neurotransmitter, the presence of cold exogenous drug that binds to the same receptor as the tracer and reduces the concentration of available receptor sites can be imaged. This scenario is diagrammed in Figure 8. An essential element of occupancy studies

http://dx.doi.org/10.5772/57414

is that there must exist a tracer that binds selectively to the desired drug target. On the other hand, the *drug* need not be selective. The change in binding of the PET tracer will reflect the occupancy of the drug only at the tracer's target. Again, occupancy of specific receptor binding sites is saturable and reduction in BP (i.e., increase in drug occupancy) increases less and less for given increases in drug as the concentration gets higher and higher. We typically define change in BP as a percentage change:

$\Delta BP = [1 - BP(\text{under a challenge condition}) / BP(\text{at baseline})]^* 100.$

For the case of an exogenous drug binding to target sites, it turns out, Occupancy = ΔBP.

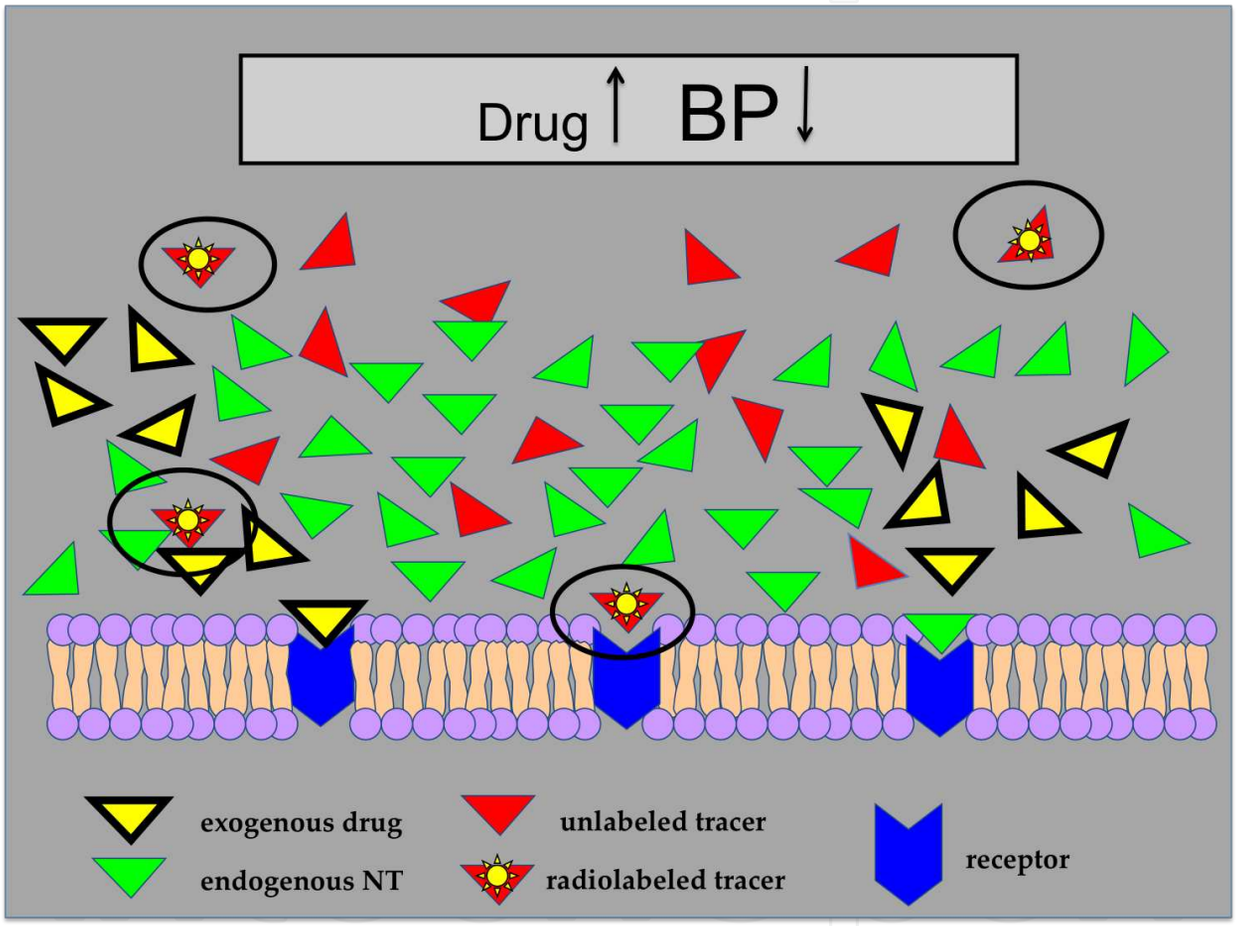

Figure 8. Effect of exogenous drug on binding potential. Drug (yellow triangles) occupies some receptor sites reducing available binding sites and then reducing BP.

1.2.8. Ambiguities in interpretation of PET data

The flexibility of BP as an endpoint of PET studies with neuroreceptor ligands (as stated, one can measure receptors, transmitters, drugs) is also the source of potential ambiguity in interpretation. How can one tell the difference between lower receptor density under scan condition B vs. A from higher neurotransmitter level in scan condition B vs. A? These ambi-

guities are inherent in the compound parameter, BP. Generally, they can be resolved by considering the context of the measurement. If a stimulus was given just before the scan and the BP was lower than at baseline, we interpret this to mean that neurotransmitter levels rose due to the stimulus. We reject receptor up-regulation as the explanation, because it is a slower process than the time-scale of the PET scan (1-2 hours). On the other hand, if baseline scans are repeated on the same individuals after a year of psychotherapy and the average BP value is higher in the latter scan, we interpret this to mean that receptor number is increased by psychotherapy. (We must admit that long-term depression of baseline neurotransmitter level is also a valid interpretation.) Certainly we can say that "available receptor sites" were increased with therapy. In all cases, one must be alert to alternative interpretations of BP and ΔBP and try as best as possible to control for them via appropriate study designs.

1.2.9. Common confounding conditions in PET experiments

Some sources of ambiguity in the interpretation of BP measurements are inherent in the nature of PET data, but others can and should be controlled experimentally.

1.2.9.1. Effect of age

The densities of many neuroreceptors are known to decline with normal aging and this has been confirmed with PET (E. D. Morris et al., 1999). Thus, BP will be lower in a group of healthy control subjects with a higher mean age than a second group whose mean age is younger. Similarly, there may be no effect of a treatment or condition (e.g., long-term drug abuse) on the numbers of a particular receptor, but it might appear so if the drug abusers have a mean age that is older than the mean age of the healthy subjects to whom they are being compared. Any careful reading of journal articles reporting BP values for different cohorts must include checking to make sure that the ages of the respective groups are not different. Similarly, a longitudinal study examining the effect of long-term treatment on a single group of individuals should correct for aging of the subjects if the length of the study is considerable.

1.2.9.2. Effect of mass

As we saw above, an exogenous drug that occupies the target receptor reduces available binding sites for the tracer, and BP is reduced. This is the basis for drug occupancy studies. However, if the specific activity of the tracer (ratio of activity to mass) is low enough, then mass of cold tracer acts like any exogenous drug. This poses two problems. First, we normally do not want the tracer species to exert its own drug effects. Second, the mass of cold tracer – as with any exogenous ligand for the target site – will occupy an appreciable number of receptors and the measured BP will be lower than if the mass of tracer were negligible. Unwanted drug effects notwithstanding, poorly controlled mass of tracer has the potential to introduce a confound into an experiment. If a patient group is being compared to a control group but the patients receive a significantly higher mean tracer mass (i.e., lower specific activity for the same amount of radioactivity injected), then the patients will appear to have lower BP due to their disease, when in fact, the difference may be caused solely by a bias introduced by experimenters.

http://dx.doi.org/10.5772/57414

1.2.10. Experimental approaches to estimate binding potential

There are generally two approaches to estimating BP and by extension, change in BP. Both approaches turn on recognizing that BP represents a steady state quantity: the ratio of bound to free tracer in the tissue at steady state – that is, when the ratio of these quantities is not changing on a macroscopic level. To make such a measurement, one can either perform an experiment that brings the pools of bound and free tracer to steady state or, if that is not possible or not desired, one can predict the steady state from non-steady measurements. If these ideas seem unintuitive, consider the two fun experiments depicted in Figure 9 for predicting the steady state (i.e., adult) height of one's daughters. Steady state approach: one can make a few measurements (greater reliability than a single measurement) once the child reaches her adult height (Figure 9, left). Non-steady approach: one can make periodic measurements throughout childhood and – given a model of growth patterns of women in the United States – *predict* the adult height of the child based on these non-steady measurements (right).

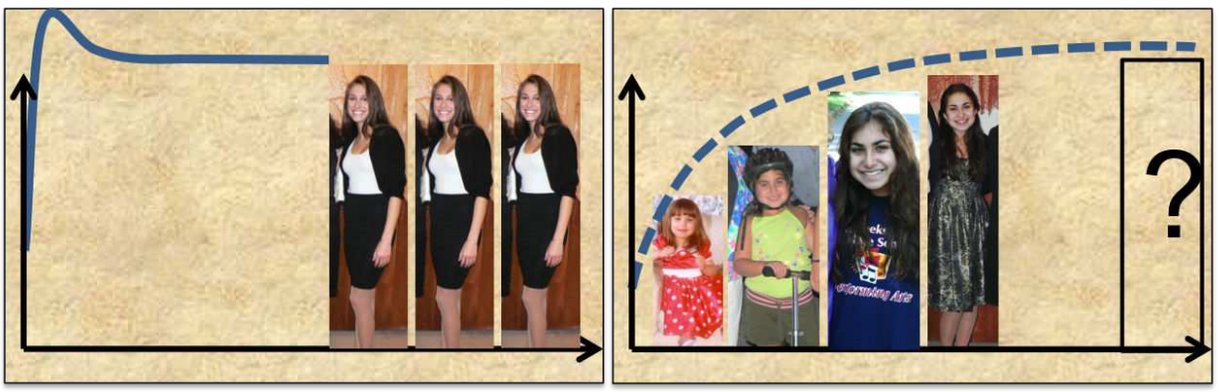

Figure 9. Schematic for (left) a type of steady state experiment for *measuring* height of a fully grown female child, as compared to (right) a type of non-steady experiment for *predicting* the adult height of the female children of one of the authors.

1.2.10.1. Bolus plus constant infusion

In PET, the steady state or equilibrium approach to measuring BP consists of administering the tracer as an initial bolus followed by a constant infusion of additional tracer for the duration of the experiment. If the bolus and infusion fractions of the tracer are balanced correctly, the TAC in the region(s) of interest will achieve a steady state in a minimal amount of time (Carson et al., 1993) at which point tracer concentrations in plasma, free and bound compartments will remain in constant proportions to each other. At said point, BP can be measured directly from the levels of the plasma and tissue curves without the need for a model or any curve-fitting. It must be pointed out that infusions are more taxing experimentally. An infusion pump is required. More tracer is required (as compared to a bolus injection), since some of it decays while sitting in the syringe waiting to be infused. Not all tissue regions are the same. Tissue regions with differing kinetics of tracer uptake will reach equilibrium at different times – or not at all. Not all subjects are the same. For a given injection protocol, one subject's tissue curves might reach equilibrium but another's might not.

1.2.10.2. Bolus studies

Alternatively, if an infusion experiment is impractical, a bolus administration of tracer is used. This approach includes a bolus injection of tracer, a dynamic acquisition of PET data, and a kinetic model to fit the data, estimate parameters, and calculate BP from the estimated model parameters. The parameters of the kinetic model are rate constants (they each have units of $time^{-1}$), but their ratio is an equilibrium (i.e., steady state) constant (BP is unitless).

Both experimental designs (bolus and bolus/infusion) can be used to measure the change in BP. In the case of the bolus administration, two separate injections are required to measure change in BP (ΔBP) – perhaps in response to a drug challenge. A single bolus plus infusion (B/I) study can suffice to measure ΔBP provided the drug challenge of interest acts rapidly enough and the tracer is sufficiently displaceable so that the effect can be detected during the duration of the scan. The two different paradigms for measuring ΔBP are diagrammed in Figure 10. Each paradigm has advantages and disadvantages that the investigator must consider carefully when planning a study (Table 1). The order of a paired bolus study (baseline vs. challenge condition) can be randomized; the B/I cannot. Both scans of a paired bolus studies with 18F-labelled tracers cannot both be performed on a single day. This may lead to greater variability in the data or even loss of some subjects who fail to return for a second scan. Equilibrium must be reached before the drug challenge in the B/I design. Unfortunately, there is no way of knowing that equilibrium has been achieved in a subject before giving the drug challenge, since PET data are not reconstructed and analyzed in real time. Finally, on the side of the B/I paradigm, the analysis of the data – provided equilibrium has been reached – is simple and requires no modeling and no curve fitting. For bolus studies, with some rare exceptions, one must use a kinetic model to describe the data in order to estimate BP.

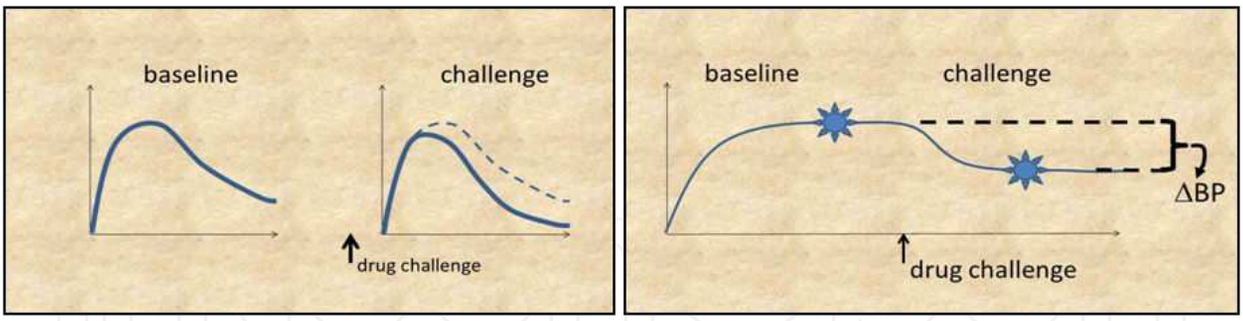

Figure 10. Two common schemes for measuring change in BP with PET. General appearance of data from a paired bolus study (left) compared to a single bolus plus infusion study (right). Stars on right indicate that only two static measurements are necessary to get change in BP from an equilibrium study

1.2.11. Modeling basics (to get to binding potential via bolus or bolus + infusion)

As we discussed in Section 1.2.3 and diagrammed in Figure 4, the PET signal consists of tracer molecules in different pools, only one of which is the specific binding we are most interested in. These pools or compartments differentiate themselves over time. They have different temporal characteristics based on their degree of retention of the tracer. The PET signal can be

Paired Bolus design	Bolus plus Infusion design
order of conditions can be randomized: baseline/ challenge	requires no model-fitting to estimate BP, ΔBP
requires two successful syntheses	requires only one successful synthesis of tracer
studies with [18F]-labeled tracers require two separate scan days; more chance of physiological variability	requires computerized injection
	(high- and low-binding) regions don't all reach equilibrium at same time.
	requires that regions of interest reach equilibrium; data may be unusable if equilibrium is not achieved
	B/I scan needs more radioactivity than single bolus scan

Table 1. Experimental Design. Some common advantages (blue) and disadvantages (red) of paired bolus and bolus plus infusion designs for measuring drug-induced changes in the neurotransmitter levels with PET.

dissected into its constituent parts with the use of a kinetic model that describes the processes of uptake and retention of the tracer, as well as the interconnectedness of the compartments.

1.2.11.1. The modeling process

The process of moving from some knowledge of the system of interest to a tracer kinetic model is diagrammed in Figure 11. One must first identify the organ(s) of interest. In the case of imaging drugs, the organ, naturally, is the brain. Next one must consider the relevant (neuro)chemistry of the selected organ and how it relates to the tracer to be used. In a simple conception of the brain, we must include the vasculature that delivers the tracer to the tissue. The blood brain barrier – how does the tracer traverse it? Once inside the tissue, are there receptors or transporters to (specifically) bind the tracer? If there are multiple possible specific binding sites, is there one site that is likely to dominate? Inevitably there will be nonspecific (i.e., non-displaceable) binding as well, because there are other entities in the tissue that appear to retain foreign molecules. Due to mathematical limitations (related to the limits of parameter identifiability), most models will treat the nonspecific binding pool as a sub-pool of the free, unbound tracer; nevertheless, we must keep in mind that such a process lurks under the surface even if it is not explicated in the model statement. Next, we must conceptualize the possible fates of the tracer into distinct pools or compartments of the model (all compartments are pools, but not all pools are compartments – see next section for explanation). Every route by which tracer can move from one compartment to another must be assigned a rate constant (designated by an arrow in Figure 11c). Finally, we turn a diagram of connected pools into a series of equations. Because what drives movement of tracer is mass action (diffusion from pools of high concentration to low), we must write mass balance equations for each compartment. Mass balance equations assert that the net accumulation of tracer over time is equal to the amount of tracer coming into the compartment per time, minus the amount of tracer leaving per time, plus tracer generated, minus tracer destroyed. Typically, generation does not apply – our bodies do not create exogenous compounds. These equations take the form of ordinary

differential equations. The only dependent variable is time. The dependent, or "state", variables are the unknown concentrations in the respective compartments.

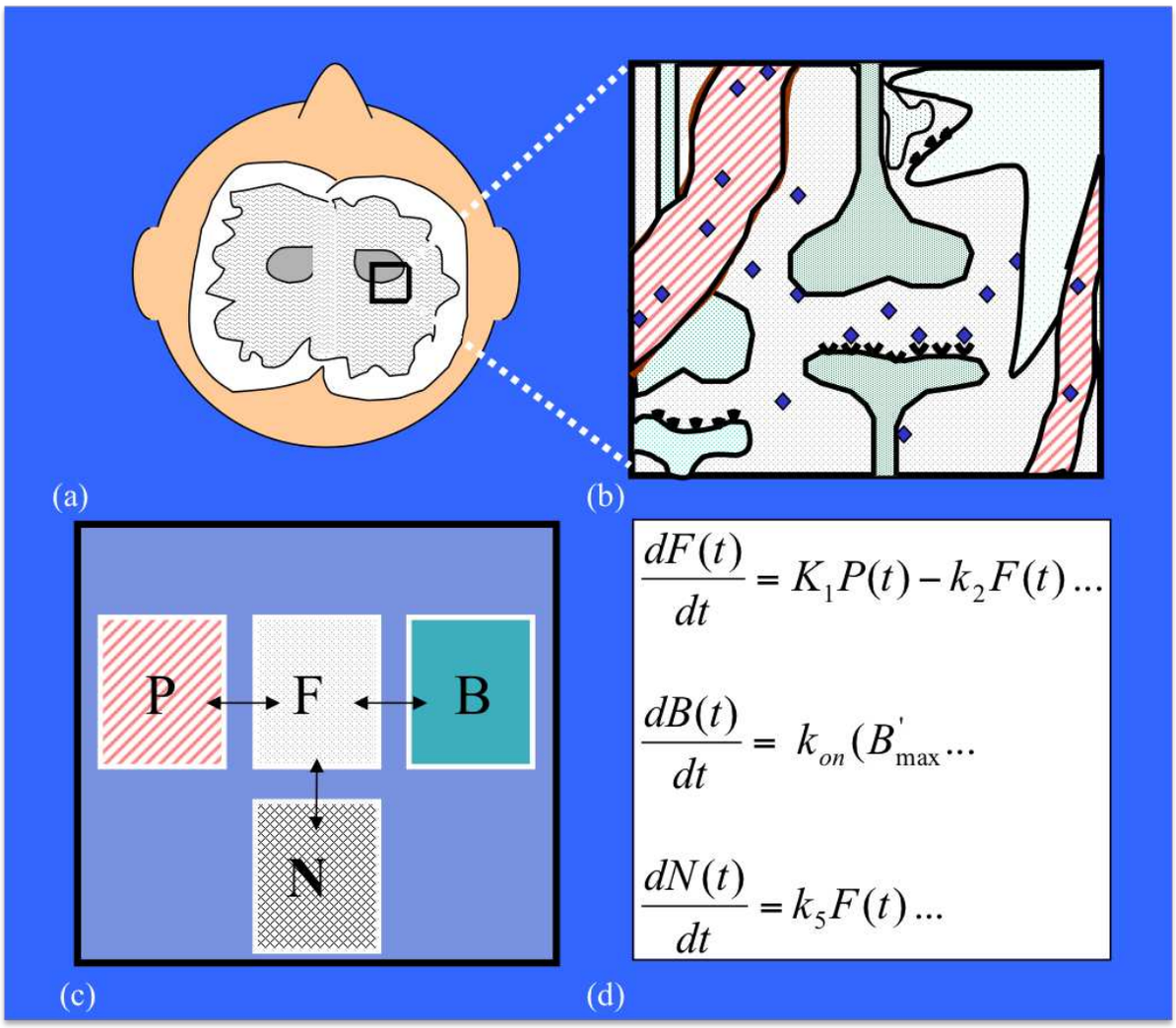

Figure 11. Schematic of the tracer kinetic modeling process. (a) Identify an organ of interest and a region of interest within it. (b) Consider the relevant physiology or biochemistry. (c) Abstract the tracer pools into connected compartments. (d) Write the mass balance equations

1.2.11.2. Compartmental models (1T, 2T)

Compartments represent the unknown variables of a model (free tracer, F, bound tracer, B). These are sometimes referred to as "state" variables. Although in most circumstances plasma-borne tracer can be thought of as a distinct "pool", we typically do not assign it a compartment, because it is measured directly via an arterial catheter and therefore not an unknown. Rather, the plasma tracer concentration over time is an input to the system. That is the case for the two most common compartmental models used to describe PET tracers: the one-tissue compartment (1T) and the two-tissue compartment (2T) models (see Figure 12). Each of these models requires measurement of the arterial plasma concentration of tracer as the input function.

http://dx.doi.org/10.5772/57414

Arterial blood taken from the arm is considered a good representation of the tracer concentration in arterial blood reaching the brain at each moment in time. For tracers that are known to bind specifically to a target, it would seem natural to model them with the 2T model. However, the 2T model has 4 unknown parameters: K_1, k_2, k_3, k_4. By contrast, the 1T model has one variable, the concentration of tracer in the tissue and only 2 parameters, K_1 and $k_2{}^{1T}$. Note that the k_2 parameters have different meanings for each of the two models and so in this chapter, we give them different superscripts to distinguish between them (the reader is advised that this is typically not done in the PET literature). While the 2T model would seem the intuitive choice – especially if we know that specific binding of tracer to a target occurs - it is not always supported by the data. That is, the specific binding may be too fast to allow for reliable estimation of k_3 and k_4 or it represents only a small fraction of the total uptake or perhaps the signal to noise ratio of the data is poor. Whatever the reason, if we cannot uniquely identify all the parameters of the 2T model by fitting it to the data, the 1T model can be used and the total volume of distribution, $V_t = K_1/k_2{}^{1T}$, becomes the estimated endpoint. By contrast, V_t as measured with the 2T model is defined as $V_t = K_1/k_2{}^{2T}(1 + BP)$. If the V_t is estimated from parameters of the 1T model, but specific binding exists, then $k_2{}^{1T}$ implicitly contains effects of the specific binding term, BP.

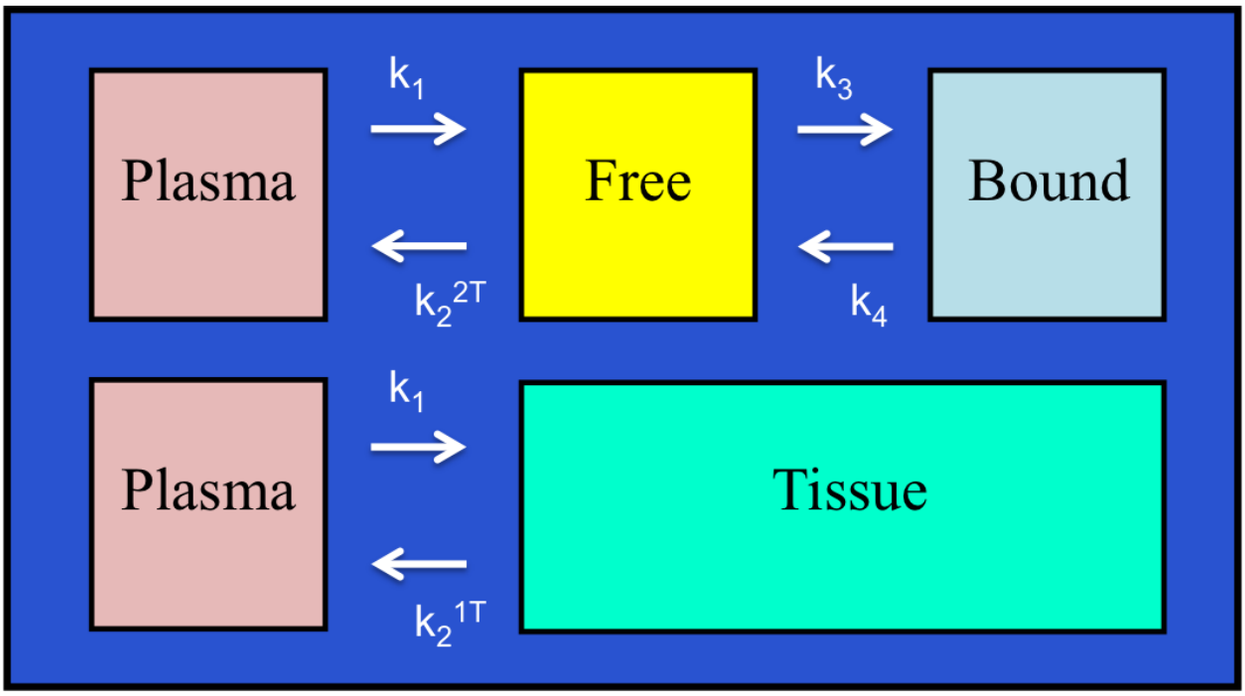

Figure 12. Common compartmental models used to analyze PET TACs. 2T model (top) has 2 unknown variables and 4 parameters (rate constants) to be estimated from the data. 1T model has only one variable (the tissue compartment) and 2 rate constants to be estimated.

1.2.11.3. Graphical methods

To fit TACs with the 1T or 2T models requires an iterative algorithm and some knowledge of numerical methods, parameter estimation, and computer programming. There is a popular

alternative to iterative curve fitting that can be used in many circumstances. Collectively, these methods are based on rearrangements of the model equations to yield linear relationships between measured quantities (Ichise et al., 2003; Logan et al., 1996; Logan et al., 1990; Patlak et al., 1985; Patlak et al., 1983; Zhou et al., 2006). One can think about these methods as transformations akin to a logarithm that transforms an exponential relationship into a linear one. The Logan plot was the first linearization of the 2T model to be applied widely to reversibly bound tracers (e.g., [11C]raclopride). The slope of the original Logan plot is equivalent to the volume of distribution, V_t, the same parameter that can be estimated directly with either the 1T or 2T model (Logan et al., 1990). An advantage of using the Logan plot is it is possible to perform all the necessary calculations in a spreadsheet. Further, the estimate of V_t via the Logan plot is highly robust. That is, it almost never fails to produce an estimate with high precision. A disadvantage of the Logan plot is that it is not unbiased. It has been shown to underestimate V_t with increasing noise in the PET data (Slifstein et al., 2000). As with proper experimental design, one must be cognizant of potential biases that can be introduced into the analysis by the model or the model transform and guard against misinterpretation.

1.2.11.4. Reference region methods

From the diagrams in Figure 12, it would appear that one always needs a measured plasma input function to drive a kinetic model. On its face, this makes sense, since tracers enter (are inputted) into the system via the plasma. In fact, models designed to describe the data in the tissue can also work with input functions derived from reference regions in the image. A reference region is one that is essentially equivalent to the target region except that it is devoid of specific binding sites. By taking advantage of the fact that the same plasma concentration of tracer supplies both the target and the reference regions, it is possible to eliminate the plasma concentration from the model and describe the concentration in the target region compartments in terms of the reference region concentration. In effect, the reference region has become the input function. This concept was first applied to PET data by Farde et al. and by Cunningham et al. (Cunningham et al., 1991; Farde et al., 1989). Subsequent assumptions applied by Lammertsma and Hume reduced the number of parameters in the reference tissue model (thus named the "simplified reference tissue model" (SRTM)) (A. Lammertsma et al., 1996; A. A. Lammertsma et al., 1996). Finally, Gunn et al. devised an implementation of SRTM (using basis functions) that turned it into a linear model and thus almost as easy to use in practice as the Logan plot (Gunn et al., 1997).

1.2.12. Physics basics

The spatial precision of PET is based on the concept of "electronic collimation". That is, radioactive decays lead to pairs of 511KeV photons being emitted in (nearly) opposite directions. When they are captured simultaneously by detectors in the PET scanner ring, a coincidence is recorded. Because of the co-linearity of the paths of the two photons, the direction from which they came is known and physical collimators (used to filter out photons approaching at various angles to the detector) are not needed. The sequence of coincidence detection is diagrammed in Figure 13. But there are certain common ways that electronic

http://dx.doi.org/10.5772/57414

collimation can be foiled and standard corrections must be applied to the raw data to assure that the emission images are quantitative and proportional to concentration of tracer. Some common artifacts that require correction are diagrammed in Figure 14 (counter-clockwise from top left).

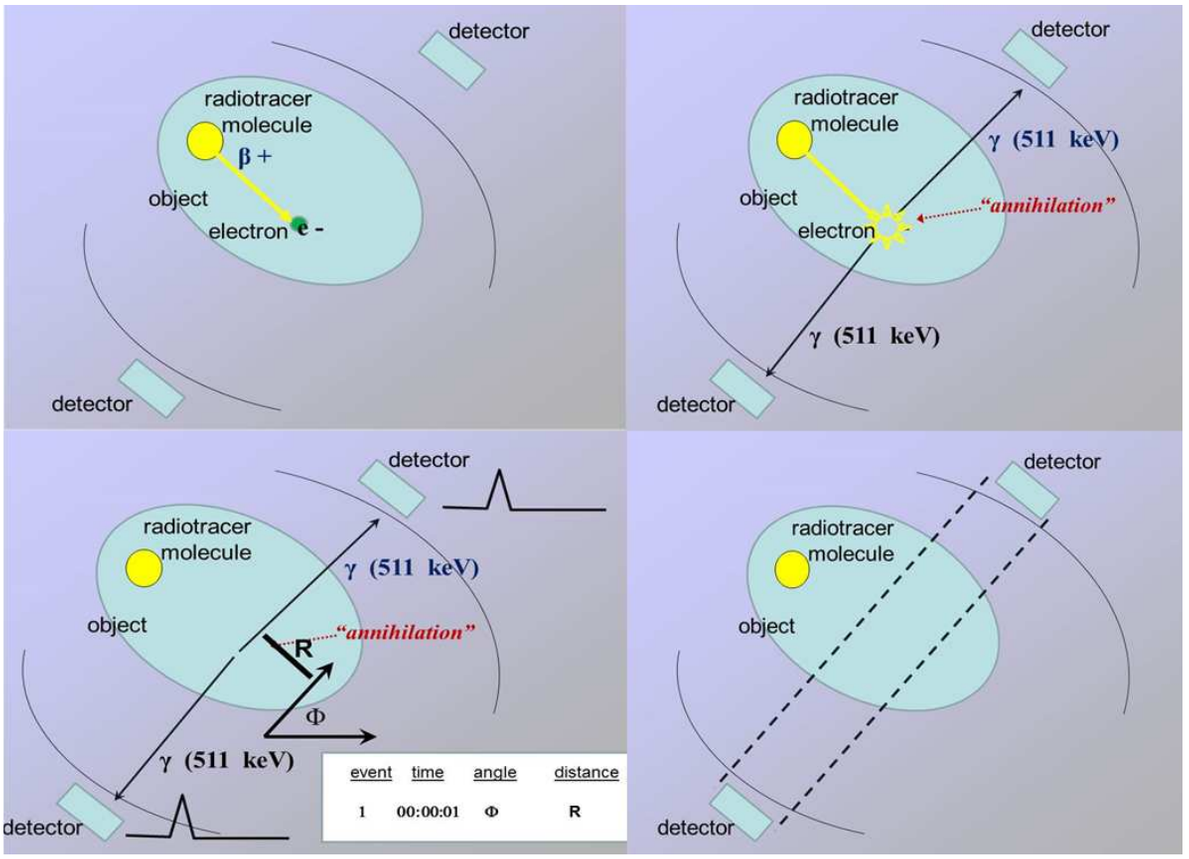

Figure 13. (top left) A positron emitter emits a beta particle. (top right) Beta particle annihilates with an electron and two photons are produced which exit the object in opposite directions. (bottom left) The two 511 KeV photons are detected by opposing detectors, leading to signals being recorded. Coincidence logic determines that the events happened within a pre-set time window. The time of the coincidence event and its unique angle, Φ, and distance, R, are recorded. (bottom right) Image reconstruction locates the original annihilation event along a line-of-response (within the dotted lines).

1.2.12.1. Scatter

If either pair of photons emanating from a single annihilation event is deflected from its path but still detected simultaneously with the non-deflected photon, then the positioning of the line of response (between the two detectors) will be incorrect.

1.2.12.2. Randoms

If one photon each from two separate annihilation events is lost to attenuation or scatter and the remaining photons (from different events) are detected simultaneously, the apparent coincidence event will be located improperly.

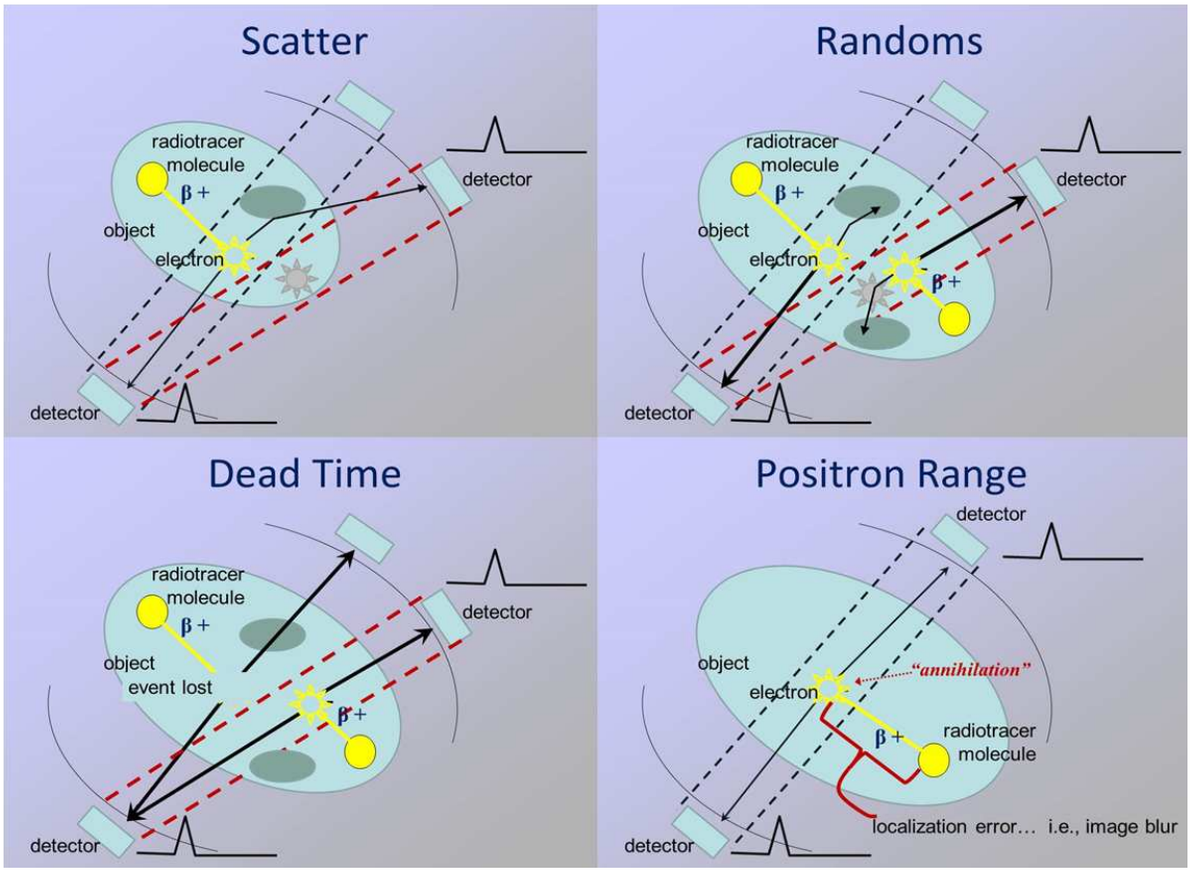

Figure 14. (a) Scatter: A collision of one of the daughter photons with scattering material disrupting the normal co-linearity of the photon paths but not their ultimate detection leads to a mis-placement of the line of response (grey start). (b) Randoms: if single photons are absorbed or otherwise not detected, unrelated pairs of photons can be detected as a coincidence leading to a mis-location of the originating event (grey star). (c) Dead Time: if too much radioactivity is in the object such that detectors cannot keep pace with decay events, then information is lost and radioactivity is no longer proportional to tracer concentration. (d) Positron Range: notice that the relocation along a line of response is never tied to the tracer molecule but rather the annihilation even though, in fact, we seek to locate tracer molecule itself. The positron range of a beta particle is inversely related to its energy and represents an unavoidable blurring of the image from ideality.

1.2.12.3. Deadtime

If the amount of radioactivity in the object is so great that the rate of annihilation events exceeds the capacity of the detectors to record them, then annihilation events will be lost. This condition threatens the quantitative value of PET. We assume that detected coincidences are proportional to concentration of radiotracer molecules in the object. If the detectors are "maxed out", then this desired linear relationship no longer holds and the images are no longer quantitative.

Commercial PET scanners typically come with reconstruction software that corrects for scatter, randoms, and deadtime.

1.2.12.4. Positron range

When a beta emitter ejects a beta particle, the particle travels some finite distance before annihilating with an electron. The two 511 KeV photons that result from the annihilation are

thus emitted from a location that is some distance from the location of the tracer molecule that we seek to localize. This distance, called the positron range, is an average distance that is dependent on the energy of the emitted beta (see Table 2). Positron range contributes uncertainty to the localization of the deposited radiotracer. Because it is not directional (equally likely for beta to travel in any direction), the positron range contributes a blur to the image.

Nuclide	$T_{1/2}$ (min)	Photon Energy (keV)	Positron Energy (MeV)	Positron Range (mm in H_20)
^{15}O	2.1	511	1.70	1.5
^{13}N	10.0	511	1.19	1.4
^{11}C	20.3	511	0.96	1.1
^{18}F	109	511	0.64	1.0

Table 2. Beta energies for common PET isotopes and their positron range

1.2.13. Attenuation correction

Without attenuation correction, regions of an object near its outer surface would appear hotter than regions deep inside because photons emerging from within a body are more likely to be scattered or absorbed and not detected than those starting on or near the body's surface. Data from a CT scan or model can correct non-uniform attenuation in the brain.

1.2.13.1. Attenuation correction artifacts

A lot of work has gone into improving attenuation correction for whole body images. Consider PET images of the chest. There are large translations of the chest from the beginning to the end of the normal respiratory cycle. Unlike CT imaging which is very fast, we cannot ask subjects to hold their breath for 10 minutes while we acquire an FDG-PET scan of their torso. In fact, the development of PET/CT (two scanners integrated together) was driven in part by the need to have multiple attenuation scans for different phases of the respiratory cycle. Kinahan and colleagues have shown – quite persuasively – that failure to align the transmission scan to data from separate 'gates' (images acquired in different phases of breathing, gated -or triggered - by the respiratory signal) causes serious artifacts on images of the chest (Liu et al., 2009). These artifacts can be so serious that they can be mistaken for tumors (Liu et al., 2009) or as serious defects in cardiac perfusion (Alessio et al., 2007). Alessio et al. showed that perfusion was underestimated by 60% if the attenuation map was misaligned due to normal respiration (Alessio et al., 2007).

Generally, a skull does not expand and contract like a chest (due to respiration), so a single transmission scan taken at the beginning or end of a PET scan session is adequate for attenu-

ation correction of brain images. However, this may not be the case for certain types of studies of drug taking (reviewed below). In these cases, the act of taking a subject out of the scanner and then re-positioning them following drug administration could potentially lead to a mismatch between the transmission scan (taken at start of session) and the PET images acquired after the re-positioning.

2. PET Imaging of drug challenge studies

Here, we discuss a series of parameters or conditions that make it challenging to use PET to image receptor changes and drug-induced changes in the human brain. These themes will be repeated throughout the remainder of the chapter as they arise in the discussions of the literature.

2.1. Novelty

Many different imaging groups measure drug-induced changes in dopamine release in the scanner or during the study day. However, dopamine is released in response not just to drugs of abuse but also to stress and to novelty. As the majority of subjects in these studies will not have been exposed to these experimental situations in their past, the experience will be novel to them. Suffice to say, it would not be helpful to be imaging novelty-induced dopamine release when one is trying to measure the effect of a drug. One way to avoid this common confound is to expose the subject to the study environment before their participation begins. In the case of our smoking-in-the-scanner studies, we have the subjects lie down in the scanner and simulate smoking at a session prior to a real scan session.

2.2. Order effects

Order effects can occur in any scientific study. In rodent studies of drug treatment when a placebo is compared to an active drug, the conditions are counter-balanced so that some rats receive the drug first and other rats receive the placebo first. This eliminates bias that could occur if the order in which drugs were given were to alter the results. In imaging studies, this can be more challenging. When using radiotracers with short half-lives (carbon-11 has a 20.3 minute half-life), it is possible and sometimes preferable to do baseline and drug-challenge scans on the same day. This can reduce the variation between scans that may occur if scans are conducted far apart in time. It also increases the likelihood that the subject will be able to easily complete the study (e.g., it is usually easier for a subject to commit to one day at the PET center rather than having to take off multiple days from their job or school). However, this also makes it more difficult to randomize the order of scans.

Consider scans of amphetamine-induced dopamine release. Amphetamine's effect on dopamine (and thus 11C-raclopride binding) is profound and long-lasting. It is not possible to do the drug-challenge scan on the same day before the baseline scan, since the effect of amphetamine would persist for hours (possibly longer) and corrupt a subsequent "baseline" meas-

urement. On the other hand, if effects of a drug or other stimulus are short-lived, it is generally possible to counter-balance the scans.

2.3. Expectation and reward-prediction error

We can learn from the work of Shultz and colleagues that dopamine neurons not only are activated in the presence of most drugs of abuse but that they are activated even before delivery of a drug, in response to cues and other stimuli that are "conditioned" or a conditioned stimulus (CS) (Schultz et al., 1997). Additionally, the dopamine neurons are sensitive to changes and errors in reward, which can be called prediction error. Dopamine neurons in the nonhuman primate brain fired after presentation of a reward that was not paired with a CS. When the reward and CS were paired, the dopamine neurons fired in response to the presentation of the CS and not to the subsequent presentation of the reward (Figure 15). That is, the dopamine neurons activated to the CS itself, because it was *predictive* of a reward (Doyon et al., 2005; Doyon et al., 2006). When the CS is presented and then the reward does not occur (negative prediction error), there is the typical activation to the CS, but then a dip in dopamine neuron activation when the expected reward does not occur. This study highlights how sensitive the dopamine system is to cues and expectation of reward, and care needs to be taken to design PET studies that take this sensitivity into account.

2.4. Sex differences

Sex differences are evident in many psychiatric disorders, medical disorders, and also in the normal human brain (Cosgrove, Mazure, et al., 2007). There are sex differences in structure (e.g., total volume of the human brain and some subdivisions), in function (e.g., emotional processing as measured with fMRI), and in chemistry (as measured with PET). These differences are important to measure, as they may clarify the clinical literature. It might be helpful, for instance, to know if the higher prevalence of depression in women vs. men can be explained by greater serotonergic dysfunction in women. Unfortunately, sex differences can also cloud the interpretation of data - if they are not carefully recognized and controlled. In one of our own studies, we were at first convinced of differences in nicotinic Acetylcholine receptor (nAChR) availability between healthy men and women when looking at a standard imaging outcome measure, volume of distribution (V_T). On further examination, however, we also found significant differences in total parent of the radiotracer (total unmetabolized radiotracer in the blood) and in f_p (the fraction of radiotracer free in the blood and not bound to plasma proteins). When these two factors were included in the analysis (by use of the normalized outcome, V_T/f_p), the apparent sex difference disappeared (Figure 16) (Cosgrove, Mitsis, et al., 2007).

2.5. Patient management

Care must be taken in managing any study with human subjects, especially patients who are not typical healthy controls but may be individuals suffering from psychiatric disorders. There is a balance that must be struck between designing a study to answer every possible experimental question and keeping the demands on the participants within reason. As described

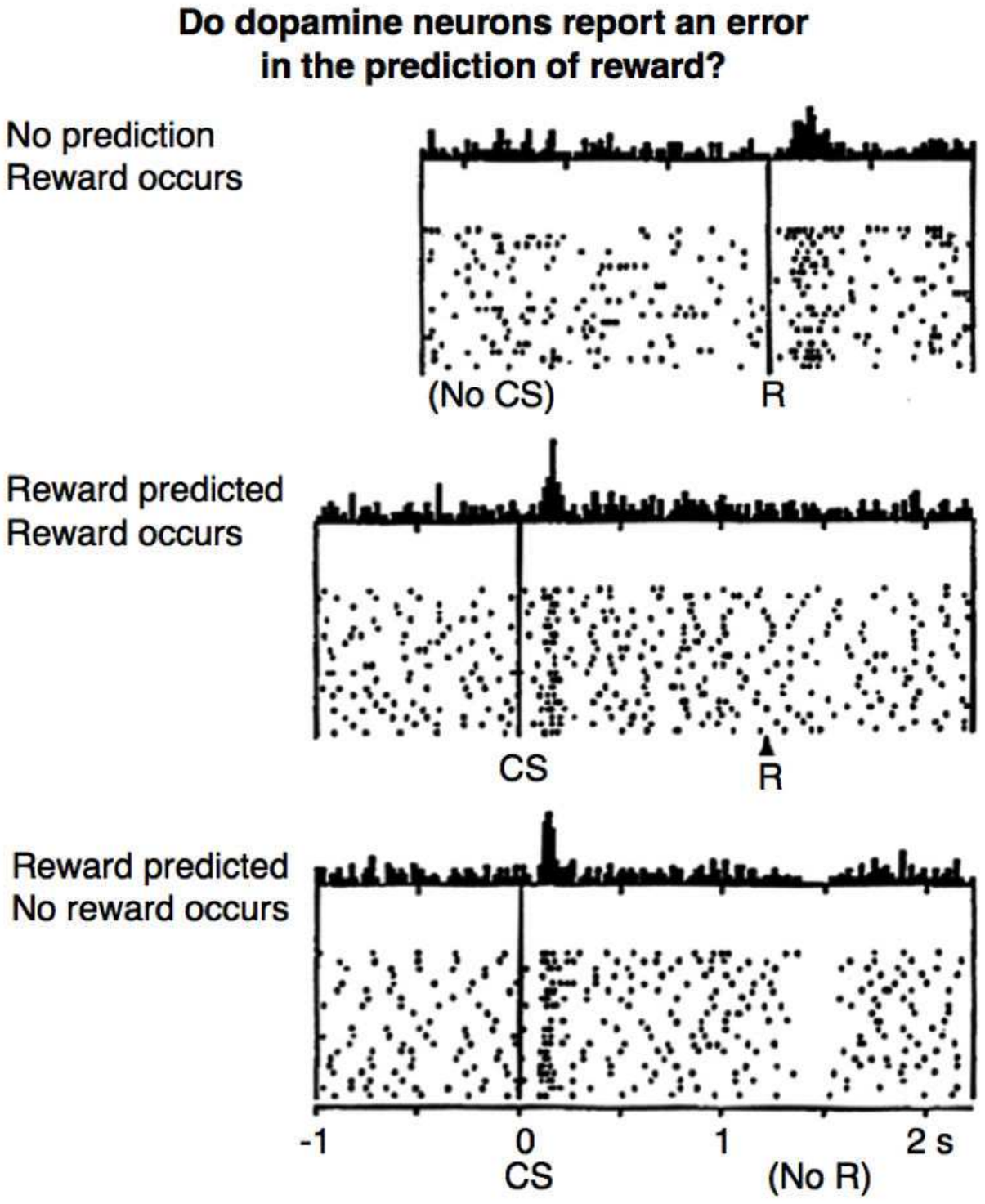

Figure 15. (Top) Prior to conditioning, reward without prediction causes a positive error in reward prediction, which increases DA neuron firing. (Middle) Following conditioning, the CS predicts the reward, leading to no prediction error. CS but not reward shows increase in DA neuron firing. (Bottom) After conditioning, CS but no reward causes a negative error in reward prediction. The CS causes increase in DA neuron firing, but the lack of reward causes a DECREASE in DA firing (Schultz et al., 1997).

http://dx.doi.org/10.5772/57414

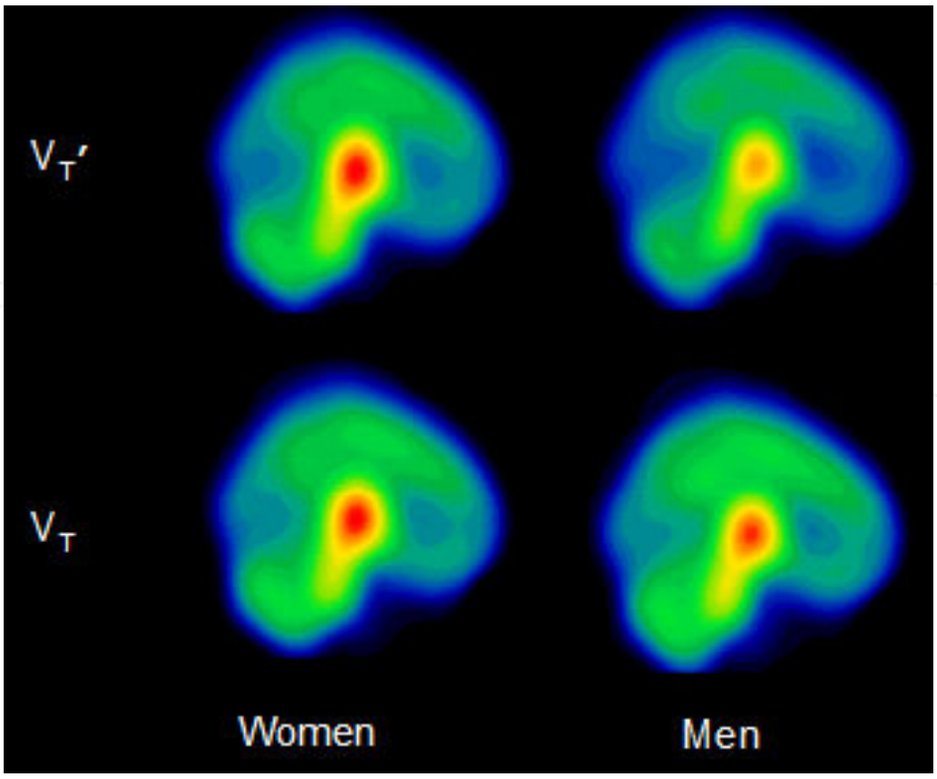

Figure 16. Mean parametric images illustrating ^{123}1-5-IA-85380 activity in 10 men and 19 women in VT' (regional activity divided by total plasma parent between 6 and 8 h) and VT (regional activity divided by free plasma parent between 6 and 8 h). Across brain regions, the main VT' component was significantly greater in women than in men, but the main VT component did not significantly differ between the sexes. This research was originally published in *JNM*. 123I-5-IA-85380 SPECT Imaging of Nicotinic Acetylcholine Receptor Availability in Nonsmokers: Effects of Sex and Menstrual Phase. JNM. 2007;48:1637. © by the Society of Nuclear Medicine and Molecular Imaging, Inc.

below, in many smoking studies we asked our subjects to quit smoking. If this is for a short time, the subjects can manage. When it is for longer, we must implement strategies to help them quit. When we asked *schizophrenic* smokers to quit smoking, we took the additional step of having them stay in an inpatient facility for the week so they could be monitored.

There is also a huge effort that goes into subject recruitment and screening before individuals are invited to participate in studies. Subjects undergo batteries of psychological tests, thorough medical evaluations including a physical exam, complete blood tests, drug toxicology tests, electrocardiograms to ensure cardiac health, and structural MRs to rule out any obvious brain abnormalities. There is also a lengthy informed consent process that must be conducted with all potential subjects. SPECT and PET studies are complex and may involve a variety of risks including administration of radiotracers, placement of arterial lines, and drug administration. Each facet of the study demands discussion between investigator and subject of the potential risks. All of our studies are carefully evaluated and approved by a local radiation safety and a human subjects investigation committee (the latter is typically referred to as an Institutional Review Board or IRB).

	Brody (2004)	Brody (2006)	Barrett (2004)	Scott (2007)
Tracer	[^{11}C]raclopride	[^{11}C]raclopride	[^{11}C]raclopride	[^{11}C]carfentanil & [^{11}C]raclopride
Injection protocol	Bolus + infusion	Bolus + infusion	Bolus	Bolus + infusion
Tracer dose	Slow bolus injection 5 mCi, followed by infusion 3mCi/hr	Slow bolus injection 185 MBq, followed by infusion 111 MBq/h	10 mCi in 10 ml saline over 120 seconds	10-15 mCi
Scanner (resolution)	ECAT 953 (5.6 mm FWHM)	GE Advance NXi	ECAT HR+ (42 mm FWHM)	Siemens HR+ (~5.5 x 5.0 mm FWHM)
Design	Inter-subject (1 scan)	Inter-subject (1 scan)	Intra-subject (2 scans)	Intra-subject (2 scans)
Analysis	Equilibrium	Equilibrium	SRTM	Logan Ref
Phenomenon to test	DA release in ventral striatum due to smoking	Gene variants of DA pathway & smoking	DA release due to smoking and hedonic response	μ-opioid and DA D2 receptors and nicotine
Subjects	20 nicotine dependent (5 female)	45 tobacco-dependent smokers	10 right-handed, non-medicated smokers (5 male)	6 right-handed, healthy male smokers; 6 age- and sex- matched controls
Subject characteristics	≥15 cigarettes/day	• 15-40 cigarettes per day • No overlap with previous study group	Minimum of 2 DSM-IV criteria for nicotine dependence	15-20 cig/day
Time from last cigarette	2 hrs	3 hrs	Minimum 12 hrs	~12 hrs
Protocol	During the scan, subjects had a 10 min break OUTSIDE scanner; 10 smoked 1 cigarette; 10 controls	During the scan, subjects had a 10 min break OUTSIDE scanner; 35 smoked 1 cigarette; 10 controls	2 scans, 1 control and 1 smoking; smoked in scanner prior to tracer delivery	Tracer infusion (randomized order), smoke 2 denicotinized cigarettes, 45 min, smoke 2 average nicotine cigarettes
Timing	10 min break (smoking or not) 50 min post scan initiation	1 hr scan, 10 min break in outdoor area (smoke/no smoke), 30 min scan	Cigarette 15 min pre [^{11}C]raclopride; aimed to smoke 1 cig / 12 min, max. 6 cigs	90 min scans; smoked each cig for 5 min; smoke denicotinized cig at 2 & 12 min; smoke avg. nicotine cig at 40 & 50 min
Self admin.	Yes, outside scanner	Yes, outside scanner	Yes, in scanner	Yes, in scanner
Cigarette type	Usual brand	Either usual brand or standard study cigarette	Usual brand	Denicotinized & average nicotine
Ventral striatum	-4.3 ± 1.4%		3.12%	
Putamen	• Left -36.6% • Right -29.7%		• Anterior 2.9% • Posterior -1.59%	

http://dx.doi.org/10.5772/57414

	Brody (2004)	Brody (2006)	Barrett (2004)	Scott (2007)
Caudate / N Acc	• Left -30.5% • Right -25.9%	-8.4 ± 13.8%	-1.9%	
Basal ganglia				9.98%
Concerns	• Going outside for no-smoking group can still be a cue • Not the first cigarette of the day, perhaps not a strong response. • CT only done prior to break, not after return to scanner- possible attenuation issues • Figure 2: 2 subjects driving the effect? • Table 2: baselines are not the same in groups (smoking group higher in all regions, although not significant)	• Only one attenuation scan (following the return to the scanner) was applied to both the pre and post break scans • Some subjects smoked favorite brand, some smoked study standard cigarette • Only 10 controls vs the 35 that smoked	• Not all subjects smoked the same number of cigarettes • Some subjects reported aversive side effects which would alter hedonic ratings • Large range of ΔBP in smoking group (ventral striatum: -57% to 70%)	• Denicotinized cigarettes possibly causing negative prediction error? • Novel use of Logan graphical analysis to detect change in slope – not published elsewhere.

Table 3. Smoking Studies

	Salonen (1997)	Boileau (2003)	Urban (2010)	Yoder (2009)	Oberlin (2013)
Tracer	[^{11}C]raclopride	[^{11}C]raclopride	[^{11}C]raclopride	[^{11}C]raclopride	[^{11}C]raclopride
Injection protocol	Bolus	Bolus	Bolus + infusion	Bolus	Bolus
Tracer dose	2.89 – 3.51 mCi	10 mCi	~ 7.8 mCi	14.1 ± 0.99 mCi	14.9 ± 0.10 mCi
Scanner (resolution)	ECAT 931 (6.1 X 6.7 mm)	ECAT HR+ (4.8 x 4.8 x 5.6 mm FWHM)	ECAT EXACT HR+	EXACT HR+ (9 mm FWHM)	EXACT HR+ (9 mm FWHM effective res.)
Design	Intra-subject (2 scans)	Intra-subject (2 scans)	Intra-subject (2 scans)	Intra-subject (3 scans)	Intra-subject (2 scans)
Phenomenon to test	Acute alcohol effect on DA release in the striatum	Alcohol induced DA release	Sex differences in DA release post alcohol challenge	Alcohol & alcohol cues	Beer flavor induced DA release
Subjects	7 healthy, right-handed men	6 healthy male nonalcoholics	21 healthy men and women	8 healthy subjects (5 male, 3 female)	49 healthy male drinkers
Subject characteristics	Non drug or alcohol dependent	Nonalcoholic moderate drinkers	Nonalcoholic, 10-15 drinks/wk	Non drug or alcohol dependent; 2 FH+; 5 surpassed hazardous drinking threshold	Non drug/alcohol dependent, except 4 meeting DSM-IV alcohol dependence; 12 FH+

	Salonen (1997)	Boileau (2003)	Urban (2010)	Yoder (2009)	Oberlin (2013)
Time from last drink	~12 hrs	24 hours	Since night before	~24 hours	~48 hours
Protocol	• Drink BEFORE scan • 2 scans: 1) placebo, 2 hr break, 2) ethanol	Drink BEFORE scan, not told content of drink until this time	Scan order randomized	3 scans: 1) neutral cues/no alcohol, 2) alcohol cues predict alcohol (but infusion delayed to post scan), 3) neutral cues with unexpected alcohol (infused during scan)	2 scans, counterbalanced: 1) preferred beer flavor, 2) Gatorade® flavor
Timing	3 separate drinks of placebo (75, 65, 55 min pre bolus), bolus, scan; 2 hr break; same schedule except using ethanol	Drink for 15 min, 30 min prior to bolus	Drink for 5-10 min, 5 min prior to bolus + infusion	Neutral or alcohol cues start 2 min after bolus, maintained 15 min	Beer or Gatorade flavor sprays (~15 ml) start 2 min after bolus, maintained 15 min
Mode of alcohol administration	Self	Self	Self	Investigator (IV infusion)	N/A
Alcohol type	Orange juice plus either tap water or ethanol	Orange juice with or without alcohol	Cranberry & soda with alcohol (~3 drinks worth) or trace alcohol	Ringer's lactate with or without alcohol	N/A
Ventral striatum		16.8 ± 16.3%	• Men: -12.1 ± 8% • Women: -6.2 ± 8%	• Cue condition w/ expected intoxication: -0.20 ± 0.1 • Unexpected alcohol condition: 0.12 ± 0.08	• R ventral striatum: • FH+: 11.7 ± 4.1% (SE) • FH (ambig.): 3.8 ± 2.5% • FH-: 2.7 ± 2.7%
N. acc.		15.0 ± 15.9%			
Putamen	No significant difference:	5.2 ± 17.5% Ventral 13.7 ± 17.5%			
Caudate	-0.10 ± 0.12 (P = 0.43)	4.0 ± 16.4%			
Concerns	•Alcohol taken long time prior to scan. • Ethanol condition aversive to subjects? (1 subject too nauseous to have > 1 drink)	•Alcohol taken long time prior to scan. • Subjects drank large amount of alcohol – may have been aversive	• Biased to find greater ΔBP: control condition (smelling alcohol but not receiving any) may have caused negative prediction error	• No conditioning to cues (ala Shultz et al 997). Study assumes that cues are salient.	• Only FH+ subjects showed effect of beer flavor on DA • Lack of resting baseline makes definitive determination of effect direction difficult

Table 4. Alcohol Studies

	Weerts (2008)	Weerts (2011)
Tracer	[^{11}C]carfentanil & [^{11}C]methyl naltrindole	[^{11}C]carfentanil & [^{11}C]methyl naltrindole
Injection protocol	Bolus	Bolus
Tracer dose	[^{11}C]CAR (19.4 ± 2.1 mCi); [^{11}C]MeNTI (19.2 ± 3.2 mCi)	Avg. mCi: [^{11}C]CFN: 19.30 (AD), 19.99 (HC); [^{11}C]MeNTL: 18.87 (AD), 17.52 (HC)
Scanner (resolution)	GE (2 x 2 x 4.25 mm)	GE (5.5 x 6.1 mm FWHM)
Design	Inter-subject	Inter-subject
Phenomenon to test	Naltrexone occupancy of ***δ***- and μ- opioid receptors	***δ***- and μ- opioid receptor availability at baseline
Subjects	21 alcohol dependent & healthy control (15 male, 6 female)	25 alcohol dependent & 30 healthy control
Subject characteristics	60+ drinks/month, at least 5 drinks/occasion weekly	DSM-IV criteria for alcohol dependence; controls <8 drinks/wk women, <15 for men
Time from last drink	15 days prior to naltrexone treatment	5 days
Protocol	15 days abstinence, followed by 4 days naltrexone	2 PET scans in fixed order on the same day: [^{11}C]MeNTL followed by [^{11}C]CFN
Timing	19 days inpatient, 50 mg p.o. 2x on day 15, then 1x daily for remainder of days; scan day	5 days inpatient protocol; scans on day 5
Mode of alcohol administration	N/A	N/A
Alcohol type	N/A	N/A
Ventral striatum	All ROIs: [11C]CAR: 94.9 + 4.9% occupancy	• AD = 1.826 ± 0.068 • HC = 1.438 ± 0.061
Putamen	[11C]MeNTI: 21.1 + 14.49% occupancy	• AD = 1.272 ± 0.044 • HC = 0.962 ± 0.040
Caudate		• AD = 1.395 ± 0.057 • HC = 1.113 ± 0.052

Table 5. Weerts Studies of Alcohol Dependence

3. Preclinical imaging of nicotinic acetylcholine receptors

3.1. Using nonhuman primate studies to aid in design of human studies

3.1.1. Wash-out of nicotine in the brain

One key way that nonhuman primate (NHP) studies can help us to inform our clinical studies is to work out basics of experimental design before we inject radiotracers into humans. For imaging studies we conducted with the goal of measuring nicotine-induced "upregulation"

of nAChRs in humans, preceding NHP studies played a critical role in experimental design. There is a wealth of literature showing that nicotine and tobacco smoking upregulate nAChRs throughout the brain (Abreu-Villaca et al., 2003; Breese et al., 1997; Kassiou et al., 2001; Marks et al., 1992). Nicotine studies with various doses and routes of administration to rats, mice, and monkeys - as well as postmortem human studies – have all demonstrated that nicotine and tobacco smoke result in significantly more nAChRs throughout the brain compared to saline (animals) or to not smoking (humans). We now know that nicotine itself is responsible for this upregulation. Nicotine acts in the cell to help the receptor subunits assemble and then acts to chaperone the receptors to the cell membrane (Srinivasan et al., 2010). Our goal was to measure this upregulation in living human tobacco smokers (Staley et al., 2006). But first, we needed to work out the proper experimental timing.

Nicotine and our radiotracer, [^{123}I]5-IA-85380, both bind to the same receptor in the brain – the nAChR containing the β2-subunit. When nicotine is present in the brain, it blocks the receptor and prevents the radiotracer from binding. Our preclinical experiment consisted of two monkeys drinking nicotine (diluted in water and sweetened with Tang to make it more appetizing) for 6 weeks. After 6 weeks, the monkeys were taken off nicotine. One monkey was scanned at 1 day into nicotine withdrawal, and the other was scanned at 2 days into nicotine withdrawal. Surprisingly, the data showed a *decrease* in radiotracer binding - suggesting that receptors may have been down-regulated! To probe further, we put the monkeys back on nicotine for two weeks and then scanned them both at 7 days of withdrawal. At that point, we saw the robust increase in radiotracer binding that was suggested by the preclinical literature. Taken together, the early data and the 7-day data suggested that nicotine remains in the brain during early withdrawal, and one must wait about 7 days for it to clear before measuring nicotine-induced upregulation. We also measured urine cotinine (the major metabolite of nicotine) levels in the monkeys over the 7 days of withdrawal. Cotinine progressively declined over the week, not completely clearing or reaching nonsmoker levels until 7 days of abstinence. The cotinine data nicely mirrored the brain closely. Once cotinine had cleared, we knew that we could proceed to measure nicotine-induced upregulation of nAChRs in the brain. In our human studies, discussed below, we routinely use low cotinine levels as an indicator that nicotine has cleared and that smokers can be scanned for nAChR.

3.1.2. Simplifying the analysis of nAChR availability

As described in the Introduction, a reference region simplifies the estimation of receptor availability. β2-nAChRs are widely distributed throughout the whole brain with highest density in the thalamus, moderate binding in the cerebellum, striatum and brainstem, and low binding throughout the cortex. There is no region in the brain completely devoid of β2-nAChRs, so there is no appropriate reference region. For many of the studies imaging β2-nAChRs with SPECT or PET described herein, a bolus plus constant infusion paradigm was used to achieve equilibrium between the brain and the blood (see Section 1.2.10.1). The outcome measure was volume of distribution, V_T, which can be calculated as concentration of radioactivity in brain divided by concentration of radioactivity in blood, provided an equilibrium has been achieved between tissue and blood concentrations of tracer. V_T is related to

http://dx.doi.org/10.5772/57414

binding potential (BP) and can be used as a measure of receptor availability. Because the bolus plus constant infusion paradigm in these studies reliably achieves equilibrium, the analysis is simplified, and there is no need for kinetic modeling. We refer to our outcome measure as receptor "availability", because we are not measuring all receptors. We cannot measure those receptors which, on average, are occupied by the endogenous neurotransmitter, acetylcholine, or by an exogenous ligand such as nicotine (hence the unexpected results at day 1 of withdrawal) (Staley et al., 2006).

3.1.3. Human nAChR scans in tobacco smokers

Based on the preclinical monkey studies, our group imaged β2-nAChRs in human tobacco smokers at 7-9 days of smoking abstinence ('withdrawal'). In these studies, the subjects were required to quit smoking and not use any medications or nicotine replacement strategies such as the patch, because all forms of nicotine would bind the β2-nAChR and block the radiotracer from binding. In order to help the subjects quit smoking, we used contingency management (Staley et al., 2006). Put simply, subjects met with a member of the research group one to two times per day and gave evidence that they had not smoked. 'Evidence' is established by carbon monoxide breath readings less than 11 parts per million (the level of a nonsmoker) and urine cotinine levels that are at the level of a nonsmoker or decreased from the day before. *Contingent* upon successful tests, subjects are paid small sums of money, and they can typically earn up to $230 for abstaining for up to 9 days. In other words, we used *positive* reinforcement to help the subjects maintain abstinence for the duration of the study. In our first paper, we demonstrated that tobacco smokers at 7-9 days of abstinence have significantly higher β2-nAChR availability in the cortex, striatum, and cerebellum compared to a group of age- and sex-matched nonsmokers (Figure 17). This work confirmed that it is possible to measure the upregulation phenomenon in human smokers, *in vivo* (Staley et al., 2006).

There is also evidence from preclinical and postmortem studies that the β2-nAchRs do not stay upregulated but return to control levels. A postmortem study indicated that smokers who had quit smoking at least two months prior to their death had β2-nAChR levels similar to controls (Breese et al., 1997). However, smokers in the study had quit anywhere from 2 months to 30 years prior to their death, so the study did not shed light on the acute time course of receptor changes, e.g., during acute withdrawal in the first few months of abstinence. In our next study, we imaged β2-nAChR changes over the first few months of abstinence in tobacco smokers (Cosgrove et al., 2009). As shown in Figure 17, at one day of abstinence, nicotine is still present in the brain blocking the receptor, and there is no difference in β2-nAChR availability compared to the group of nonsmokers. At one week of abstinence, we again demonstrate there is higher β2-nAchR availability in smokers compared to nonsmokers. Then even at 2 and even 4 weeks of abstinence, receptor availability remains high and does not return to nonsmoker control levels until 6-12 weeks of abstinence. This study demonstrates that upregulation of β2-nAChRs is persistent, and these brain changes during acute abstinence are consistent with the clinical course of smoking cessation in which craving, relapse, and withdrawal symptoms occur over the first few months of abstinence, and relapse may occur months or years after the last cigarette. It is possible that nicotine replacement strategies are effective in some people,

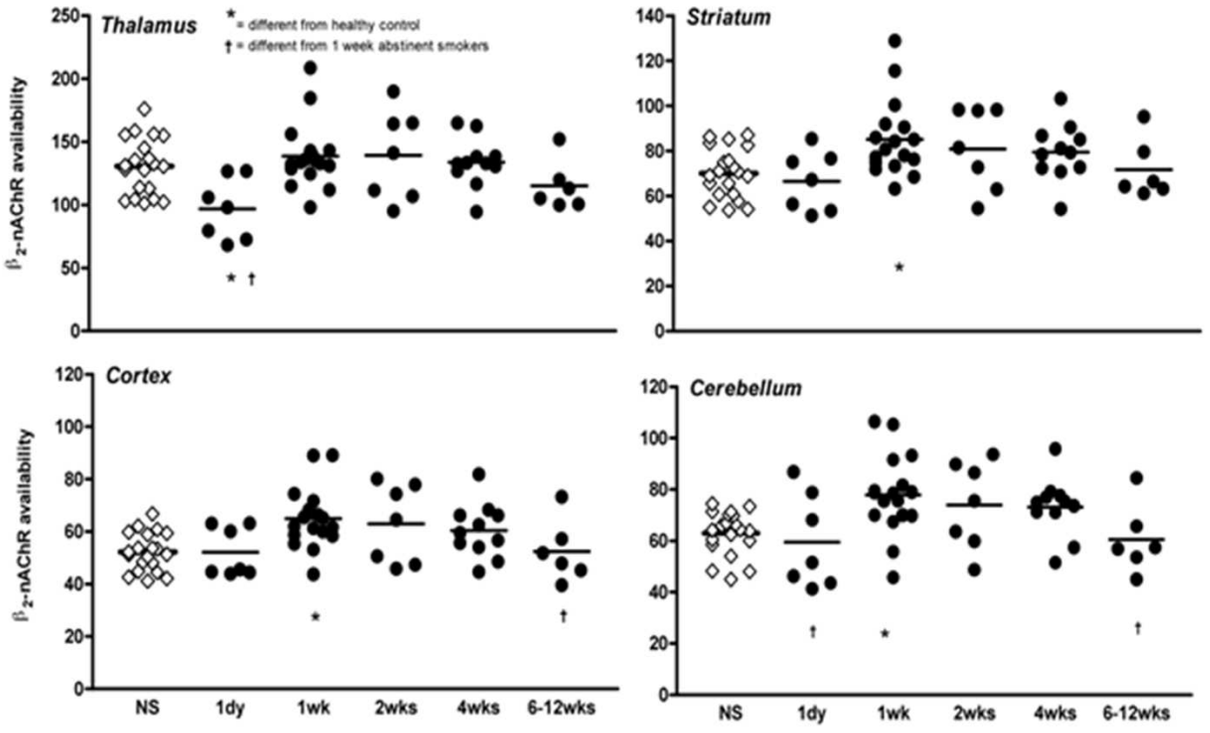

Figure 17. β_2-nAChR availability (V_T/f_p) is shown in individual nonsmokers (open diamonds) and tobacco smokers (filled circles) at 1 day, 1 week, 2 weeks, 4 weeks, and 6-12 weeks of abstinence in the thalamus, striatum (average of caudate and putamen), cortex (average of cortical regions including parietal, frontal, anterior cingulate, temporoinsular, and occipital cortex), and cerebellum. The line in each scatter plot represents the mean value of those subjects. * indicates significant difference from control nonsmokers after Bonferroni's correction using two-sample t-tests. † indicates significant difference from 1 week abstinent smokers after Bonferroni's correction using planned post-hoc between-group comparisons subsequent to the analysis of repeated measures mixed-effects regression models including the overall effect of abstinent smoker group.

because they continue to activate the pool of upregulated receptors and help "wean" the receptors off of nicotine as the dose of nicotine is decreased over time.

There is a large literature demonstrating sex differences in tobacco smoking behaviors. In general, men tend to smoke for the nicotine reinforcement, or nicotine *per se* in the cigarette, whereas women tend to smoke more for the sensory cues associated with smoking, as well as affect and stress regulation (Perkins, 2009; Perkins et al., 1999; Perkins et al., 2008). There are also two preclinical studies showing that male rats and mice exposed to nicotine exhibited greater nAChR upregulation than female rats and mice exposed to nicotine (Koylu et al., 1997; Mochizuki et al., 1998). We wanted to determine if there were sex differences in β2-nAChR availability between men and women smokers compared to nonsmokers. Consistent with the preclinical literature, we found that male smokers had significantly higher β2-nAChRs compared to male nonsmokers (between 9 and 17%) but that women smokers had similar β2-nAChR availability compared to women nonsmokers (between 1 and 3 %) (Cosgrove et al., 2012). This was a striking finding given all the studies demonstrating that nicotine and tobacco smoking upregulate β2-nAChRs throughout the brain. Considering known behavioral sex differences in tobacco smoking, these findings make sense and provide

a biological mechanism that may underlie some of the behaviors. Specifically, men smoke for the nicotine in cigarettes, they are more responsive to nicotine replacement therapy as a cessation strategy, and men's brains are responsive to nicotine, exhibiting upregulation of β2-nAChRs. Women smoke for affect regulation and for reasons other than the nicotine, they do not respond as well to nicotine replacement strategies, and their brains do not respond to nicotine by increasing β2-nAChRs. The bottom line is that novel treatment strategies targeting other receptor systems need to be evaluated to more effectively help women quit smoking. All the current strategies act at the β2-nAChR, and, of course, all nicotine replacement strategies act at that site. Varenicline (Chantix) is a partial agonist at the β2-nAChR, and even bupropion (Zyban) is a nicotinic antagonist.

In addition to receptor changes, imaging studies have informed our knowledge about what happens in the brain after someone smokes a cigarette. For example, after one puff of a cigarette, approximately 50% of all β2-nAChRs in the brain are occupied by nicotine. After smoking one or two cigarettes, the receptors are saturated, so 100% of β2-nAchRs are occupied by nicotine (Brody, Mandelkern, London, et al., 2006). We know that nicotine doesn't clear the brain right away, so if all the receptors are occupied by nicotine, why do people keep smoking throughout the day? This brings up some important points about tobacco smoking. People smoke for many different reasons, and nicotine reinforcement is only one component. The reinforcement or pleasure derived from nicotine, like many other drugs of abuse, is necessary in driving the initial phases of drug seeking behavior. But as the addiction progresses, many people continue to smoke in order to avoid withdrawal symptoms and due to the many conditioned cues that have become ingrained, which are a part of the repetitive nature of tobacco smoking. Additionally, there are 4000 chemical compounds that are produced when a cigarette burns; all of these compounds are in tobacco smoke and are inhaled. Thus, while nicotine is the primary addictive component of tobacco smoke, there are additional compounds such as MAO-A and MAO-B inhibitors that likely play a role.

Other imaging studies have demonstrated that even smoking a denicotinized cigarette, which supposedly has very low nicotine content, still occupies up to 20% of β2-nAChRs in the brain (Brody et al., 2008). This is similar to the level of occupancy produced by second hand smoke. Dr. Arthur Brody and colleagues at UCLA performed an elegant study examining the effect of second hand smoke on β2-nAChRs by having subjects sit in a car (the window was down a few inches) with a person smoking, and they reported up to 20% of β2-nAChRs were occupied by nicotine in the individual who was just sitting in the car, not smoking (Brody et al., 2012). Interestingly, a recent law in California prohibits smoking in the car with children under the age of 18.

3.1.4. Use of microdialysis measurements

Before PET made possible indirect measurement of dopamine release, *in vivo*, the only way to measure dopamine levels in a living brain was via microdialysis. Microdialysis is used primarily in rodents. During a surgery, a probe is placed through the skull into the region of interest, e.g., the nucleus accumbens. After recovery, dopamine levels can be sampled in the awake, behaving animal typically in response to a drug or a stimulus. Di Chiara and Imperato

performed the seminal study showing that drugs abused by humans release DA in the nucleus accumbens of the rat brain using this technique (Di Chiara et al., 1988). Amphetamine (1.0 mg/kg, SC) raised DA levels over 1000% from baseline, whereas ethanol (1.0 g/kg, IP) and nicotine (0.6 mg/kg, SC) raised DA levels to 200% over baseline levels. This illustrates how powerful DA release can be when it is directly stimulated as with amphetamine, which is both a direct DA releaser and DA reuptake inhibitor. Put into context, a similar dose of amphetamine given to a monkey or a human in a PET experiment, which is an indirect measure of change in DA, would result in a 15-30% change in BP as measured with [^{11}C]raclopride or another D2/3 ligand.

4. Imaging dopamine release in response to nicotine, tobacco smoking, and alcohol in humans

As we have recounted, one natural strategy for using PET and SPECT to study smoking has been to image nAChR directly with a nicotinic ligand. Such studies have led to greater understanding of nicotine's persistence in the brain, sex differences in nAChR levels, and the role of nicotine in up-regulation of those levels. There is a second way that molecular imaging techniques can shed light on the neurochemistry of smoking (and drinking). As suggested by microdialysis studies, the mesolimibic DA system is important as the common pathway through which all drugs of abuse – and other rewarding inputs - are processed. With PET and a dopaminergic ligand that competes with DA for binding to a receptor, one could, in theory, image the effects of reward processing in the brain in response to an addictive substance or behavior. In practice, such studies have proved quite challenging and the reader must take care to consider the strengths and weaknesses of each attempt. One challenge is that neither alcohol nor nicotine causes large elevations of DA levels above baseline – probably only a doubling or tripling of baseline. And, the effects of both drugs are short-lived. A third challenge is that self-administration of the substances by a volunteer (smoking a cigarette, drinking a beer) is not easily performed within the confines of the PET scanner.

4.1. Nicotine and tobacco smoking

Most of the PET studies of the dopaminergic response to cigarette smoking and/or nicotine are summarized in Table 2. Barrett et al. did one of the earliest studies of smoking with PET; the first study with smokers actually smoking in the scanner (Barrett et al., 2004). The tracer was [11C]raclopride, a D2 antagonist that has been found to be sensitive to changes in endogenous DA (Dewey et al., 1993; Seeman et al., 1989). Barrett et al. used the paired-bolus design described in Figure 10 (left). But instead of administering the stimulus (i.e., smoking a cigarette) prior to the tracer, subjects were asked to smoke repeatedly (six times!) while in the scanner for the one-hour smoking scan. No task was performed during the baseline scan. The authors did not find any significant change in raclopride binding potential from baseline in any areas of the striatum when they looked at the results of all 10 smokers together. The study was, however, characterized by very large variation in ΔBP across smokers (range in ventral striatum: [-57%, 70%]). When the subjects who experienced "mood elevating effects in response

http://dx.doi.org/10.5772/57414

to [ ] smoking" (n=5) were broken out from the complete cohort, the authors found a 21% decrease in BP from baseline (i.e., increase in DA) in the caudate.

There were some notable innovations in the Barrett et al. study as well as some reasons for caution in interpretation. On the plus side, the smokers smoked in the scanner - thus any DA release detected could be attributed to the entire smoking behavior – something not possible with animals but highly relevant for medications development. The smokers were asked to smoke their own brand - another way of assuring that behavior in the scanner approximated subjects' smoking behavior. The authors recognized that, strictly speaking, the comparison of a baseline BP to one measured under a drug condition requires that a new level of DA be *constant* and maintained throughout the latter scan (we will return to this later). Because smoking probably causes only brief elevation of DA (Di Chiara et al., 1988), the investigators required repeated cigarettes – starting 15 minutes prior to tracer - in an attempt to achieve a constant elevated DA during the drug scan. Subjects were also asked to rate the "hedonic value" of their experience and their craving every 15 minutes during the smoking session. The investigators probed their data in creative and innovative ways. Across subjects (i.e., one data point per subject), they looked for correlations at every voxel in the striatum between change in BP from baseline and craving. R^2 values were then converted to t-scores, which were thresholded at $p < 0.05$. They found a relationship between craving and ΔBP in dorsal and posterior areas of striatum.

On the downside, the extreme variability in BP values suggests the possibility of motion artifact and/or resolution limitations that would preferentially mar the measurement of activity in very small regions, such as the ventral striatum. Subject motion during smoking is unavoidable and could easily explain the wild variability between subjects. The protocol of six cigarettes in an hour is overly demanding and was very likely aversive to some of the subjects. Four subjects were unable to complete the prescribed regimen of cigarettes. Needless to say, imaging of aversive stimuli was not the intended aim of the study and would have constituted a confound. In our own experience, smokers move their heads when they smoke, and they are none too happy to be asked to smoke a second cigarette *even 25 minutes after* a first.

Scott et al. took an entirely different approach to both the experimental paradigm and the analysis (Scott et al., 2007). Their experiment contained only one scan per subject, and yet it involved a bolus of tracer rather than the more standard single-scan design with a bolus plus constant infusion. Two denicotinized cigarettes were smoked in succession early in the scan at 2 and 12 minutes post injection, and two regular nicotine-containing cigarettes were smoked at minutes 40 and 50 post-tracer injection. By virtue of this design, the investigators are asking a slightly different question than in other studies, namely, what role does the nicotine in cigarettes play in DA release? The cohort was extremely small (n=6 right-handed male smokers). There was also a nonsmoker group scanned at baseline and compared to smokers under denicotinized cigarettes. The value of this comparison is questionable at best. For smokers, there was no statistically significant decrease in raclopride binding from denicotinized to nicotine-containing cigarettes in any subregion of the striatum across the six smokers. In many of the regions, the reported standard deviations of the BP estimates were quite high, and the authors would have been well served simply to scan more subjects. As in the case of

Barrett et al., the investigators looked for and found a correlation between change in BP and a behavioral (or demographic) measure (Barrett et al., 2004). In the case of Scott, the significant relationship discovered was between greater decrease in BP (so presumed greater increase in DA) from denicotinized to nicotine-containing vs. degree of dependence on nicotine (as measured by the Fagerström score) (Scott et al., 2007). In contrast to Barrett, the Scott finding was in the ventral striatum. To their credit, Scott et al. corrected their statistical tests for multiple comparisons.

As with the Barrett paper, the Scott paper involved smoking in the scanner, so motion artifacts must be considered a real possibility. Although the paper mentions motion-correction, the state of the art in 2007 would have allowed correction of misalignment between reconstructed frames acquired over minutes. Nothing could have been done about motion of the subject that happened within the duration of a single time-frame (we note that with the advent of list-mode data, high frequency motion monitoring, and interative image reconstruction algorithms, within-frame motion correction is now possible). The investigators were able to carry out a bolus design rather than a bolus plus constant infusion because of their innovative analysis technique. They employed the Logan plot, mentioned above, to linearize the time-activity curves. Their claim was that they could find two separate slopes (two measures of the ratio of Vt in the striatum to Vt in the reference region) within the plot. The first slope would reflect binding of tracer in the early phase of the scan (corresponding to the denicotinized cigarettes), and the second slope would reflect the later phase (nicotine-containing). In our hands, this technique is extremely sensitive to the choice of data-range for each slope (Sullivan et al., 2013), and we have not seen any papers in the literature subsequent to Scott either using or evaluating said technique.

Two other studies should be mentioned. Like Scott et al., they were both focused on measuring the nicotine (as opposed to cigarette) effect on DA release in humans. Montgomery et al. administered nicotine to subjects via nasal spray (Montgomery et al., 2007); Takahashi et al. had subjects chew nicotine gum (Takahashi et al., 2008). Neither group found any significant change in BP with nicotine in any individual striatal region. Takahashi showed a significant decline in [11C]raclopride binding with nicotine administration in the striatum overall. The former seems like the best design; the latter would seem to be susceptible to motion from chewing - despite express instructions to subjects to chew with their lower jaw only. Following up on Scott et al. and Barrett et al., both newer studies looked for correlations between ΔBP and behavior. Montgomery found a correlation between "happiness" and ΔBP in associative striatum. In apparent agreement with Scott et al., Takahashi found voxels in the "ventral putamen" that showed a significant correlation between raclopride ΔBP and Fagerström score.

Finally, the most oft-cited smoking studies were performed by Brody et al. This is the same group at UCLA that did the study of second-hand smoke's ability to occupy nAChR, described above. Brody and colleagues employed yet a different experimental paradigm. Smokers were scanned with an [11C]raclopride bolus plus constant infusion for 90 minutes (Brody et al., 2004). From 50 to 60 minutes, the subjects went outside for a "smoke break". All the while, they were being infused with [11C]raclopride. Ten smokers smoked a cigarette while outside; ten did not. All returned and were repositioned in the scanner and scanned for a further 30

http://dx.doi.org/10.5772/57414

minutes. The data were analyzed with an equilibrium analysis (see Figure 10) comparing BP at baseline (period just preceding smoke break) with BP after smoking (period just following smoke break). The major finding was a large (but variable) amount of DA release in ventral caudate, ventral putamen, which was statistically greater in the smokers who smoked than in those who did not. In a follow up study, the same group used the same protocol two years later, and while they replicated the direction of the findings, the effect size was quite a bit smaller (Brody, Mandelkern, Olmstead, et al., 2006). In both studies, they found that the greater the reduction of craving for a cigarette from pre- to post-break, the greater the reduction in raclopride binding potential in the ventral caudate-nucleus accumbens region. The 2006 paper introduces genetic variation and its possible role in smoking. Subjects were typed for mutations in the genes that encode for dopamine receptors, dopamine transporter or catechol-O-methyltransferase (an enzyme that breaks down catecholamines) proteins. Their results suggest that differences in amount of DA released (change in tracer binding) could be related to mutation status, and this in turn helps to explain some of the inherent variability in the BP numbers in both studies.

There are some real strengths to the UCLA design. There is also some reason for concern. First, there is no smoking in the scanner, so there is no reason to worry about smoking-related head motion. On the other hand, repositioning the smokers without taking a new transmission scan could lead to reconstruction artifacts in the post-smoke-break images (transmission and emission data not aligned). In the investigators' defense, they also scanned a control group of smokers who take their break but do not smoke. There is no reason to expect that emission-transmission misalignment would be more likely in the smokers than in the controls, so it is probably not the driver of their results. The second – and more subtle – reason for caution in interpreting the Brody et al. data requires that we first compare their findings in 2004 with those in 2006.

In the equilibrium analysis, investigators must choose a data window at the end of the pre-break data to use for a baseline measurement. In both cases, the last 10 minutes of data – from 40-50 minutes – was used. In the 2004 paper, they used 10 minutes of data post-break; in 2006, they used 30 minutes. The investigators correctly asserted in their second paper that a key assumption of their analysis is that DA must remain elevated throughout the 30 minutes post-break (this is why Barrett et al. asked subjects to smoke multiple cigarettes) (Brody, Mandelkern, Olmstead, et al., 2006). Unfortunately, this assumption must be incorrect. If it were true, then both studies should have found exactly the same change in BP. But in 2006, they found less of an effect: only 8.4% change as compared to ~30% change in 2004. The explanations offered by the authors were not persuasive: motion-induced DA release in controls, repositioning error. None of these were any more likely to have occurred in the smoking group as opposed to the control. Rather, the discrepancy between 2006 and 2004 is entirely consistent with a change in the analysis procedure that, in essence, washed out the effect by averaging over a period that contains smoking induced DA release and a subsequent period in which DA levels are returning (have returned) to baseline. In other words, they used too wide a data window in their second paper. To be sure, we recently did a simulation study of smoking-induced DA release as measured by raclopride-PET and its dependence on the selection of the

data window (Sullivan et al., 2013). While the simulations confirmed what we suspected, they raise an even more troubling concern about all previous attempts to image smoking effects on DA. That is, how can we compare across studies if people use even slightly different analysis techniques? How can we compare across groups if the time-period of response of dopamine to any drug stimulus is short and different between groups? And more generally, how can we apply standard models that assume "that DA concentration will remain elevated" to PET data when the assumption is not true? We address this important technical question in the final section of the chapter following our discussion of drinking studies.

4.2. Imaging dopamine release in response to alcohol

If smoking is difficult for subjects lying in the scanner, it is nevertheless possible. Drinking while lying in the scanner is not. Researchers have taken two approaches to this problem. The most obvious study design for measuring alcohol-induced DA release is for the subject to drink an alcoholic beverage shortly before being scanned and compare raclopride BP in this condition to either baseline or placebo. This is the approach that was employed by the three studies to look at drinking-induced DA release, per se. Salonen et al., Boileau et al., and Urban et al. each used two-scan designs (Boileau et al., 2003; Salonen, 1997; Urban et al., 2010). In each case, the conditions were either juice or alcohol plus juice. The conditions were randomized in the latter two studies. The Boileau and Salonen studies each consisted of 6 subjects; Urban scanned 11 men and 10 women. The subjects were social drinkers. The dose of alcohol was approximately 1 ml/kg in Boileau and Urban but about 1.3 ml/kg in Salonen. The blood alcohol levels in each study were consistent and generally reflected the respective doses (measurements were not taken at the same times, so direct comparisons are difficult). In any case, Urban claims that the dose in her study was equivalent to 3 standard drinks. Where the paradigms begin to diverge is the relative timing of alcohol and tracer. The alcohol was taken either 60 minutes, 30 minutes or 5 minutes prior to tracer injection in Salonen, Boileau and Urban, respectively. A second difference was that in the Urban study, the rim of the juice glass for the juice-only condition was coated with alcohol to minimize any difference in the subjects' expectation between conditions. A final noteworthy difference is that the Urban study used paired bolus plus infusion scans, whereas the other studies both used the more standard paired-bolus design.

The Salonen and Urban studies were essentially negative. No statistically significant decrease in [11C]raclopride binding was found in any region of the striatum in the alcohol condition compared to juice. Boileau reported decreases of 14-15% in raclopride BP in regions that they termed Nucleus Accumbens and Ventral Putamen. Despite finding no statistically significant drop in BP in any individual region, Urban reported a sex difference in decrease in BP in all regions taken together (see paper for further explanation). What is clear from these studies is that imaging effects of oral alcohol on DA in the striatum is not easy and that we may be at the limits of detectability for raclopride-PET. Perhaps if we scrutinize elements of each design, we may find something worth tweaking. In all studies, the amount of alcohol was quite large. Some subjects – even social drinkers – may have found it aversive. Each study reported at least one subject who dropped out. As with the smoking studies, the idea is to image drug-taking,

http://dx.doi.org/10.5772/57414

not aversion. In the Salonen study, the alcohol was taken a lengthy time before the tracer (from 75 – 55 min before). Although the authors were careful to document considerably elevated blood alcohol at both the beginning and end of the (1 hour) scanning period, one should not confuse elevated alcohol level with elevated DA. In fact, it is likely that DA responds early to drinking – possibly to the cues or the rapid rise in brain alcohol and then returns to baseline more quickly than alcohol level itself. In fact, it appears that Oberlin et al. have demonstrated that DA responds to the cues for alcohol rather than the alcohol itself (Oberlin et al., 2013). Consider nicotine. Nicotine remains in the brain for days, but the discrepancy (discussed above) between the 2004 and 2006 Brody papers (and microdialysis data) certainly suggests that nicotine-induced DA elevation is rather brief (Brody, Mandelkern, Olmstead, et al., 2006; Brody et al., 2004). All three alcohol-drinking designs suffer from lack of a baseline condition. Juice alone is used as a placebo, but if the taste of juice is rewarding then perhaps DA was released in this condition. There is always a difficulty interpreting any study that contains only placebo and drug. The difference could be due to changes during drug or changes during placebo. Consider the Urban design (Urban et al., 2010). In order to control expectation across conditions, the juice-only glass was rimmed with alcohol. But what if the smell of alcohol actually set up an expectation of alcohol? In that case, the juice condition was scanned while the subject experienced disappointment over not receiving the reward. This is called "reward prediction error" and in monkeys, it has been shown to be the cause of decreased dopaminergic firing rates as discussed previously (Schultz et al., 1997). Is there any evidence that reward prediction error leads to alteration of dopamine levels in humans? We must consider one last raclopride-PET paper to answer that question.

Yoder et al. took a different experimental approach to the study of alcohol-induced DA release (Yoder et al., 2009). Wary of the variability in alcohol absorption among people, they chose to administer the alcohol intravenously. The technique, called the "alcohol clamp", was developed by O'Connor et al. and is based on pharmacokinetic modeling of a variable-rate infusion of alcohol to maintain a constant blood alcohol level in each subject based on their height, weight, and gender (O'Connor et al., 1998). Second, expectation was controlled through visual and olfactory cues, which preceded – and predicted - the delivery of alcohol or saline, IV. There were three conditions scanned in three separate sessions – each scanned with a bolus of [11C]raclopride. The conditions were as follows: #1: neutral cues signaling IV saline, #2: alcohol cues signifying alcohol, and #3: neutral cues coupled with unexpected alcohol. This design was constructed to decouple expectation from consumption of alcohol. The alcohol in condition #2 was delivered *after* the data acquisition was complete, so the condition can be thought of "expectation of alcohol but no alcohol consumption" whereas condition #3 – thanks to a little trickery – can be thought of as "alcohol consumption with no expectation of alcohol". Subjects' answers to questionnaires during the scan confirmed that expectations were controlled as intended. The results were quite provocative: in left ventral striatum, BP of "alcohol consumption without expectation" went down relative to condition #1. That is, this comparison signifies increase in DA. But, in the contralateral ventral striatum, BP of "expectation of alcohol without alcohol consumption" was *higher* than condition #1. The authors explained this combination of results as follows. Expectation of reward without reward is equivalent to negative reward prediction error. Reward without expectation of reward is positive prediction

error. The caveat in this interpretation is that the subjects (heavy drinkers) must be considered to have been "conditioned" by their drinking history to respond with appropriate expectation to the cues. Accepting the author's interpretation, this paper highlights the importance of controlling expectation in the study of drugs of abuse. To return to the Urban design (Urban et al., 2010), if the initial smell of alcohol on the rim of the juice-only glass was a cue for imminent alcohol reward, then we might expect DA to decrease during this scan. When compared to a second condition (i.e., alcohol drink), any apparent increase in DA with alcohol could, in fact, be the result of decrease in the juice-only condition.

Finally, in this section we should point out that there are many other important lines of investigation of alcohol abuse using PET other than examining DA release. Some have looked at receptor number (Martinez et al., 2005; Volkow et al., 1996), and others have looked at change in BP due to drugs for treatment of alcohol. We highlight two studies, briefly. Both studies are by Weerts et al. (Weerts et al., 2008; Weerts et al., 2011). Both studies looked at the Mu opioid receptor (MOR) and the Delta opioid receptor (DOR) thanks to the use of two selective tracers, [11C]carfentail and [11C]methyl-naltrindol. Collectively, the two studies looked at baseline level of MOR and DOR, as well as occupancy of the receptors due to four days of treatment with naltrexone, a non-selective opioid receptor antagonist that is prescribed for alcohol abuse. Baseline receptors in alcoholics were compared to healthy controls, and occupancy of naltrexone was measured in alcoholics only. The main findings were that clinical doses of naltrexone occupied 95% of MOR but only 75% of DOR. Second, MOR and DOR levels in high binding regions of the brain were higher in alcoholics than in controls (MOR was significant; DOR was not). The first finding suggests that any variability on efficacy of naltrexone is probably not mediated by binding to MOR, since all alcoholics were uniformly blocked. The second finding suggests that years of drinking may lead to upregulation of MOR and DOR, which is more like nAChR (Cosgrove et al., 2009) and less like D2 (Martinez et al., 2005).

5. Limitations of conventional modeling methods — Need for new ones

As previously stated, the "conventional" kinetic models used in all of the work discussed to this point treat BP as a surrogate for number of receptors (because $BP = B_{max}/K_D$ where B_{max} is available, unoccupied receptors and K_D is the affinity of the tracer for the receptor.) Depending on the circumstance, investigators treat ΔBP as change in available receptors due to altered number of receptors or altered level of endogenous transmitter occupying sites. Whether the analysis method is a full fitting of dynamic data or fitting of linearized data via the Logan plot or measurement of equilibrium levels, the underlying kinetic model is the same. In all cases, however, a fundamental assumption of the model(s) is that BP is not changing over the course of the study, because BP is a constant. Mathematically, we say that the kinetic model is time-invariant in parameters. The inadequacies of all three common methods of analysis in the face of transient DA release have been thoroughly studied in the recent paper by Sullivan et al (Sullivan et al., 2013). The reader is directed to that paper for more details. Any violation of the time-invariant parameters assumption could lead to misinterpretation of data. Many if not all of the investigators whose work is profiled herein appreciate this limitation of the kinetic

http://dx.doi.org/10.5772/57414

models. As such, they asked subjects to smoke cigarettes every 15 minutes repeatedly (Barrett et al., 2004), or they were careful to assay blood alcohol level at start and end of scan and show that it was the same (Salonen, 1997). Nevertheless, no one can assure that DA remains constant throughout the PET scan. In fact, in the case of drinking or smoking, it almost certainly does not. Recall that if smoking-induced DA levels were constant in the Brody experiments, there would have been no discrepancy between the analyses of the 2004 and 2006 data sets (Brody, Mandelkern, Olmstead, et al., 2006; Brody et al., 2004). If alcohol drinking-induced DA levels were constant, there would be no discrepancy between the Boileau finding of change in BP and the Salonen negative result even though one gave alcohol 30 minutes before the scan, and the other gave it an hour before (Boileau et al., 2003; Salonen, 1997). What's more, if the timing of DA release is different across groups then – as Yoder et al. showed – the mere difference in timing could result in differences in BP and thus be interpreted as differences in magnitude of DA release (Yoder et al., 2004).

We have been working over the last ten years to develop kinetic models of tracer uptake and binding in the presence of transient neurotransmitter release (Constantinescu et al., 2007; Constantinescu et al., 2008; E. Morris et al., 1995; E. D. Morris et al., 2010; E. D. Morris et al., 2013; E. D. Morris et al., 2005; M. D. Normandin et al., 2008; M. D. Normandin et al., 2012; Sullivan et al., 2013). The earlier versions of the model were based on the idea that dopamine (or any other transmitter that competes with tracer) can exist in the free or bound states in addition to the various states of the tracer (refer back to Figures 4 and 11). New species in the model required new "boxes" which, in turn, meant more differential equations (E. Morris et al., 1995; E. D. Morris et al., 2005). The model described the data well (E. Morris et al., 1995; E. D. Morris et al., 2008) but was cumbersome to use. Subsequent work by Constantinescu and by Normandin et al. developed linearized versions of the model that could be solved quickly (and hence at each voxel) while retaining time-varying terms to describe brief changes in neurotransmitter level (M. Normandin et al., 2009). Validation of these models was carried out either (a) by configuring experiments in which a predictable pattern of DA change could be provoked in human subjects (Constantinescu et al., 2008; E. D. Morris et al., 2010), or (b) a comparison could be made between model predictions and microdialysis measurements made in the (rat) subjects at the same time as PET (E. D. Morris et al., 2008; M. D. Normandin et al., 2008; M. D. Normandin et al., 2012). Most recently, we have adapted the Normandin approach to the voxel level so that we can estimate time-courses of dopamine at each voxel in the striatum where "activation" is occurring due to drug stimulus. A critical step in such a process is some sort of statistical test to determine that change in DA really occurred at that location (voxel) in question. Finally, the outcome is a collection of curves in time at many voxels in the brain. The visualization technique that we have invented to display such 4-dimensional results is a "dopamine movie", wherein dopamine level is color-coded and the color in the activated voxels is displayed overlaid on MRI as a series of frames. The methods are described and demonstrated in a new publication in the Journal of Visualized Experiments (E. D. Morris et al., 2013). Validation and testing of these new dopamine movies is ongoing. We hope that they are a more sensitive probe of DA changes in the brain as a consequence of smoking and drinking behavior and that the increased sensitivity of the method will allow us to tease out patterns of response that are either "addictive" or "non-addictive".

Author details

Evan D. Morris, Molly V. Lucas and Kelly P. Cosgrove

*Address all correspondence to: evan.morris@yale.edu

Yale PET Center, Yale University, USA

References

[1] Abreu-Villaca, Y., F. J. Seidler, D. Qiao, C. A. Tate, M. M. Cousins, I. Thillai, & T. A. Slotkin. (2003). Short-term adolescent nicotine exposure has immediate and persistent effects on cholinergic systems: critical periods, patterns of exposure, dose thresholds. *Neuropsychopharmacology, 28*(11), 1935-1949.

[2] Alessio, A. M., S. Kohlmyer, K. Branch, G. Chen, J. Caldwell, & P. Kinahan. (2007). Cine CT for attenuation correction in cardiac PET/CT. *J Nucl Med, 48*(5), 794-801.

[3] Barrett, S. P., I. Boileau, J. Okker, R. O. Pihl, & A. Dagher. (2004). The hedonic response to cigarette smoking is proportional to dopamine release in the human striatum as measured by positron emission tomography and [11C]raclopride. *Synapse, 54*(2), 65-71.

[4] Biju, G., & R. de la Fuente-Fernandez. (2009). Dopaminergic function and progression of Parkinson's disease: PET findings. *Parkinsonism Relat Disord, 15 Suppl 4*, S38-40.

[5] Boileau, I., J. M. Assaad, R. O. Pihl, C. Benkelfat, M. Leyton, M. Diksic, R. E. Tremblay, & A. Dagher. (2003). Alcohol promotes dopamine release in the human nucleus accumbens. *Synapse, 49*(4), 226-231.

[6] Breese, C., M. Marks, J. Logel, C. Adams, B. Sullivan, A. Collins, & S. Leonard. (1997). Effect of smoking history on [^{3}H]nicotine binding in human postmortem brain. *J Pharmacol Exp Ther, 282*, 7-13.

[7] Brody, A. L., M. A. Mandelkern, M. R. Costello, A. L. Abrams, D. Scheibal, J. Farahi, E. D. London, R. E. Olmstead, J. E. Rose, & A. G. Mukhin. (2008). Brain nicotinic acetylcholine receptor occupancy: effect of smoking a denicotinized cigarette. *Int J Neuropsychopharmacol*, 1-12.

[8] Brody, A. L., M. A. Mandelkern, E. D. London, A. Khan, D. Kozman, M. R. Costello, E. E. Vellios, M. M. Archie, R. Bascom, & A. G. Mukhin. (2012). Effect of secondhand smoke on occupancy of nicotinic acetylcholine receptors in brain. *Arch Gen Psychiatry, 68*(9), 953-960.

[9] Brody, A. L., M. A. Mandelkern, E. D. London, R. E. Olmstead, J. Farahi, D. Scheibal, J. Jou, V. Allen, E. Tiongson, S. I. Chefer, A. O. Koren, & A. G. Mukhin. (2006). Ciga-

rette smoking saturates brain alpha 4 beta 2 nicotinic acetylcholine receptors. *Arch Gen Psychiatry, 63*(8), 907-915.

[10] Brody, A. L., M. A. Mandelkern, R. E. Olmstead, D. Scheibal, E. Hahn, S. Shiraga, E. Zamora-Paja, J. Farahi, S. Saxena, E. D. London, & J. T. McCracken. (2006). Gene variants of brain dopamine pathways and smoking-induced dopamine release in the ventral caudate/nucleus accumbens. *Arch Gen Psychiatry, 63*(7), 808-816.

[11] Brody, A. L., R. E. Olmstead, E. D. London, J. Farahi, J. H. Meyer, P. Grossman, G. S. Lee, J. Huang, E. L. Hahn, & M. A. Mandelkern. (2004). Smoking-induced ventral striatum dopamine release. *Am J Psychiatry, 161*(7), 1211-1218.

[12] Brooks, D. J., E. P. Salmon, C. J. Mathias, N. Quinn, K. L. Leenders, R. Bannister, C. D. Marsden, & R. S. Frackowiak. (1990). The relationship between locomotor disability, autonomic dysfunction, and the integrity of the striatal dopaminergic system in patients with multiple system atrophy, pure autonomic failure, and Parkinson's disease, studied with PET. *Brain, 113 (Pt 5)*, 1539-1552.

[13] Carson, R. E., M. A. Channing, R. G. Blasberg, B. B. Dunn, R. M. Cohen, K. C. Rice, & P. Herscovitch. (1993). Comparison of bolus and infusion methods for receptor quantitation: application to [18F]cyclofoxy and positron emission tomography. *J Cereb Blood Flow Metab, 13*(1), 24-42.

[14] Constantinescu, C. C., C. Bouman, & E. D. Morris. (2007). Nonparametric extraction of transient changes in neurotransmitter concentration from dynamic PET data. *IEEE Trans Med Imaging, 26*(3), 359-373.

[15] Constantinescu, C. C., K. K. Yoder, D. A. Kareken, C. A. Bouman, S. J. O'Connor, M. D. Normandin, & E. D. Morris. (2008). Estimation from PET data of transient changes in dopamine concentration induced by alcohol: support for a non-parametric signal estimation method. *Phys Med Biol, 53*(5), 1353-1367.

[16] Cosgrove, K. P., J. Batis, F. Bois, P. K. Maciejewski, I. Esterlis, T. Kloczynski, S. Stiklus, S. Krishnan-Sarin, S. O'Malley, E. Perry, G. Tamagnan, J. P. Seibyl, & J. K. Staley. (2009). beta2-Nicotinic acetylcholine receptor availability during acute and prolonged abstinence from tobacco smoking. *Arch Gen Psychiatry, 66*(6), 666-676.

[17] Cosgrove, K. P., I. Esterlis, S. A. McKee, F. Bois, J. P. Seibyl, C. M. Mazure, S. Krishnan-Sarin, J. K. Staley, M. R. Picciotto, & S. S. O'Malley. (2012). Sex differences in availability of beta2*-nicotinic acetylcholine receptors in recently abstinent tobacco smokers. *Arch Gen Psychiatry, 69*(4), 418-427.

[18] Cosgrove, K. P., C. M. Mazure, & J. K. Staley. (2007). Evolving knowledge of sex differences in brain structure, function, and chemistry. *Biol Psychiatry, 62*(8), 847-855.

[19] Cosgrove, K. P., E. M. Mitsis, F. Bois, E. Frohlich, G. D. Tamagnan, E. Krantzler, E. Perry, P. K. Maciejewski, C. N. Epperson, S. Allen, S. O'Malley, C. M. Mazure, J. P. Seibyl, C. H. van Dyck, & J. K. Staley. (2007). 123I-5-IA-85380 SPECT imaging of nico-

tinic acetylcholine receptor availability in nonsmokers: effects of sex and menstrual phase. *J Nucl Med, 48*(10), 1633-1640.

[20] Cunningham, V. J., S. P. Hume, G. R. Price, R. G. Ahier, J. E. Cremer, & A. K. Jones. (1991). Compartmental analysis of diprenorphine binding to opiate receptors in the rat in vivo and its comparison with equilibrium data in vitro. *J Cereb Blood Flow Metab, 11*(1), 1-9.

[21] Dewey, S. L., G. S. Smith, J. Logan, J. D. Brodie, J. S. Fowler, & A. P. Wolf. (1993). Striatal binding of the PET ligand 11C-raclopride is altered by drugs that modify synaptic dopamine levels. *Synapse, 13*(4), 350-356.

[22] Di Chiara, G., & A. Imperato. (1988). Drugs abused by humans preferentially increase synaptic dopamine concentrations in the mesolimbic system of freely moving rats. *Proc Natl Acad Sci U S A, 85*(14), 5274-5278.

[23] Doyon, W. M., S. K. Anders, V. S. Ramachandra, C. L. Czachowski, & R. A. Gonzales. (2005). Effect of operant self-administration of 10% ethanol plus 10% sucrose on dopamine and ethanol concentrations in the nucleus accumbens. *J Neurochem, 93*(6), 1469-1481.

[24] Doyon, W. M., E. C. Howard, T. S. Shippenberg, & R. A. Gonzales. (2006). Kappa-opioid receptor modulation of accumbal dopamine concentration during operant ethanol self-administration. *Neuropharmacology, 51*(3), 487-496.

[25] Farde, L., L. Eriksson, G. Blomquist, & C. Halldin. (1989). Kinetic analysis of central [11C]raclopride binding to D2-dopamine receptors studied by PET--a comparison to the equilibrium analysis. *J Cereb Blood Flow Metab, 9*(5), 696-708.

[26] Farde, L., H. Hall, E. Ehrin, & G. Sedvall. (1986). Quantitative Analysis of D2 Dopamine Receptor Binding in the Living Human Brain by PET. *Science, 231*(4735), 258-261.

[27] Gunn, R. N., A. A. Lammertsma, S. P. Hume, & V. J. Cunningham. (1997). Parametric imaging of ligand-receptor binding in PET using a simplified reference region model. *Neuroimage, 6*(4), 279-287.

[28] Ichise, M., J. S. Liow, J. Q. Lu, A. Takano, K. Model, H. Toyama, T. Suhara, K. Suzuki, R. B. Innis, & R. E. Carson. (2003). Linearized reference tissue parametric imaging methods: application to [11C]DASB positron emission tomography studies of the serotonin transporter in human brain. *J Cereb Blood Flow Metab, 23*(9), 1096-1112.

[29] Innis, R. B., V. J. Cunningham, J. Delforge, M. Fujita, A. Gjedde, R. N. Gunn, J. Holden, S. Houle, S. C. Huang, M. Ichise, H. Iida, H. Ito, Y. Kimura, R. A. Koeppe, G. M. Knudsen, J. Knuuti, A. A. Lammertsma, M. Laruelle, J. Logan, R. P. Maguire, M. A. Mintun, E. D. Morris, R. Parsey, J. C. Price, M. Slifstein, V. Sossi, T. Suhara, J. R. Votaw, D. F. Wong, & R. E. Carson. (2007). Consensus nomenclature for in vivo imaging of reversibly binding radioligands. *J Cereb Blood Flow Metab, 27*(9), 1533-1539.

[30] Kassiou, M., S. Eberl, S. Meikle, A. Birrell, C. Constable, M. Fulham, D. Wong, & J. Musachio. (2001). In vivo imaging of nicotinic receptor upregulation following chronic (-)-nicotine treatment in baboon using SPECT. *Nuc Med Biol, 28*, 165-175.

[31] Koylu, E., S. Demirgoren, E. London, & S. Pogun. (1997). Sex difference in up-regulation of nicotinic acetylcholine receptors in rat brain. *Life Sci, 61*, PL 185-PL190.

[32] Lammertsma, A., & S. Hume. (1996). Simplified referene tissue model for PET receptor studies. *Neuroimage, 4*, 153-158.

[33] Lammertsma, A. A., C. J. Bench, S. P. Hume, S. Osman, K. Gunn, D. J. Brooks, & R. S. Frackowiak. (1996). Comparison of methods for analysis of clinical [11C]raclopride studies. *Journal of cerebral blood flow and metabolism : official journal of the International Society of Cerebral Blood Flow and Metabolism, 16*(1), 42-52.

[34] Liu, C., L. A. Pierce, 2nd, A. M. Alessio, & P. E. Kinahan. (2009). The impact of respiratory motion on tumor quantification and delineation in static PET/CT imaging. *Phys Med Biol, 54*(24), 7345-7362.

[35] Logan, J., J. S. Fowler, N. D. Volkow, G. J. Wang, Y. S. Ding, & D. L. Alexoff. (1996). Distribution volume ratios without blood sampling from graphical analysis of PET data. *J Cereb Blood Flow Metab, 16*(5), 834-840.

[36] Logan, J., J. S. Fowler, N. D. Volkow, A. P. Wolf, S. L. Dewey, D. J. Schlyer, R. R. MacGregor, R. Hitzemann, B. Bendriem, S. J. Gatley, & et al. (1990). Graphical analysis of reversible radioligand binding from time-activity measurements applied to [N-11C-methyl]-(-)-cocaine PET studies in human subjects. *J Cereb Blood Flow Metab, 10*(5), 740-747.

[37] Marks, M. J., J. R. Pauly, S. D. Gross, E. S. Deneris, I. Hermans-Borgmeyer, S. F. Heinemann, & A. C. Collins. (1992). Nicotine binding and nicotinic receptor subunit RNA after chronic nicotine treatment. *J Neurosci, 12*(7), 2765-2784.

[38] Martinez, D., R. Gil, M. Slifstein, D. R. Hwang, Y. Huang, A. Perez, L. Kegeles, P. Talbot, S. Evans, J. Krystal, M. Laruelle, & A. Abi-Dargham. (2005). Alcohol dependence is associated with blunted dopamine transmission in the ventral striatum. *Biol Psychiatry, 58*(10), 779-786.

[39] Martinez, D., M. Slifstein, A. Broft, O. Mawlawi, D. R. Hwang, Y. Huang, T. Cooper, L. Kegeles, E. Zarahn, A. Abi-Dargham, S. N. Haber, & M. Laruelle. (2003). Imaging human mesolimbic dopamine transmission with positron emission tomography. Part II: amphetamine-induced dopamine release in the functional subdivisions of the striatum. *J Cereb Blood Flow Metab, 23*(3), 285-300.

[40] Mathis, C. A., B. J. Bacskai, S. T. Kajdasz, M. E. McLellan, M. P. Frosch, B. T. Hyman, D. P. Holt, Y. Wang, G. F. Huang, M. L. Debnath, & W. E. Klunk. (2002). A lipophilic thioflavin-T derivative for positron emission tomography (PET) imaging of amyloid in brain. *Bioorg Med Chem Lett, 12*(3), 295-298.

[41] Mintun, M., M. Raichle, M. Kilbourn, G. Wooten, & M. Welch. (1984). A quantitative model for the in vivo assessment of drug binding sites with positron emission tomography. *Ann Neurol, 15*, 217-227.

[42] Mochizuki, T., V. Villemagne, U. Scheffel, R. Dannals, P. Finley, Y. Zhan, H. Wagner, & J. Musachio. (1998). Nicotine induced up-regulation of nicotinic receptors in CD-1 mice demonstrated with an in vivo radiotracer: gender differences. *Synapse, 30*, 116-118.

[43] Montgomery, A. J., A. R. Lingford-Hughes, A. Egerton, D. J. Nutt, & P. M. Grasby. (2007). The effect of nicotine on striatal dopamine release in man: A [11C]raclopride PET study. *Synapse, 61*(8), 637-645.

[44] Morris, E., R. Fisher, N. Alpert, S. Rauch, & A. Fischman. (1995). In vivo imaging of neuromodulation using positron emission tomography: optimal ligand characteristics and task length for detection of activation. . *Human Brain Mapping*, 35-55.

[45] Morris, E. D., S. I. Chefer, M. A. Lane, R. F. Muzic, Jr., D. F. Wong, R. F. Dannals, J. A. Matochik, A. A. Bonab, V. L. Villemagne, S. J. Grant, D. K. Ingram, G. S. Roth, & E. D. London. (1999). Loss of D2 receptor binding with age in rhesus monkeys: importance of correction for differences in striatal size. *J Cereb Blood Flow Metab, 19*(2), 218-229.

[46] Morris, E. D., C. C. Constantinescu, J. M. Sullivan, M. D. Normandin, & L. A. Christopher. (2010). Noninvasive visualization of human dopamine dynamics from PET images. *Neuroimage, 51*(1), 135-144.

[47] Morris, E. D., S. J. Kim, J. M. Sullivan, S. Wang, M. D. Normandin, C. C. Constantinescu, & K. P. Cosgrove. (2013). Creating Dynamic Images of Short-lived Dopamine Fluctuations with lp-ntPET: Dopamine Movies of Cigarette Smoking. *J Vis Exp*(78).

[48] Morris, E. D., M. D. Normandin, & W. K. Schiffer. (2008). Initial comparison of ntPET with microdialysis measurements of methamphetamine-induced dopamine release in rats: support for estimation of dopamine curves from PET data. *Mol Imaging Biol, 10*(2), 67-73.

[49] Morris, E. D., K. K. Yoder, C. Wang, M. D. Normandin, Q. H. Zheng, B. Mock, R. F. Muzic, Jr., & J. C. Froehlich. (2005). ntPET: a new application of PET imaging for characterizing the kinetics of endogenous neurotransmitter release. *Mol Imaging, 4*(4), 473-489.

[50] Normandin, M., R. Badgaiyan, W. Schiffer, & E. Morris. (2009). A linear simplification of the parametric ntPET model for estimation of neurotransmitter response kinetics. *J Nucl Med, May*(Suppl).

[51] Normandin, M. D., & E. D. Morris. (2008). Estimating neurotransmitter kinetics with ntPET: a simulation study of temporal precision and effects of biased data. *Neuroimage, 39*(3), 1162-1179.

[52] Normandin, M. D., W. K. Schiffer, & E. D. Morris. (2012). A linear model for estimation of neurotransmitter response profiles from dynamic PET data. *Neuroimage, 59*(3), 2689-2699.

[53] O'Connor, S., S. Morzorati, J. Christian, & T. K. Li. (1998). Clamping breath alcohol concentration reduces experimental variance: application to the study of acute tolerance to alcohol and alcohol elimination rate. *Alcohol Clin Exp Res, 22*(1), 202-210.

[54] Oberlin, B. G., M. Dzemidzic, S. M. Tran, C. M. Soeurt, D. S. Albrecht, K. K. Yoder, & D. A. Kareken. (2013). Beer flavor provokes striatal dopamine release in male drinkers: mediation by family history of alcoholism. *Neuropsychopharmacology, 38*(9), 1617-1624.

[55] Patlak, C. S., & R. G. Blasberg. (1985). Graphical evaluation of blood-to-brain transfer constants from multiple-time uptake data. Generalizations. *J Cereb Blood Flow Metab, 5*(4), 584-590.

[56] Patlak, C. S., R. G. Blasberg, & J. D. Fenstermacher. (1983). Graphical evaluation of blood-to-brain transfer constants from multiple-time uptake data. *J Cereb Blood Flow Metab, 3*(1), 1-7.

[57] Pellerin, L., & P. J. Magistretti. (1994). Glutamate uptake into astrocytes stimulates aerobic glycolysis: a mechanism coupling neuronal activity to glucose utilization. *Proc Natl Acad Sci U S A, 91*(22), 10625-10629.

[58] Perkins, K. A. (2009). Sex differences in nicotine reinforcement and reward: influences on the persistence of tobacco smoking. *Nebr Symp Motiv, 55*, 143-169.

[59] Perkins, K. A., E. Donny, & A. R. Caggiula. (1999). Sex differences in nicotine effects and self-administration: review of human and animal evidence. *Nicotine Tob Res, 1*(4), 301-315.

[60] Perkins, K. A., & J. Scott. (2008). Sex differences in long-term smoking cessation rates due to nicotine patch. *Nicotine Tob Res, 10*(7), 1245-1250.

[61] Salonen, I., Hietala, J., Laihinen, A., Lehikoinen, P., Leino, L., Nagren, K., Ruotsalainene, U., Oikonen, V., Tuokkola, T., Nanto, V. (1997). A PET Study on the Acute Effect of Ethanol on Striatal D2 Dopamine Receptors with [11C]Raclopride in Healthy Males. *Human Psychopharmacology, 12*, 145-152.

[62] Schultz, W., P. Dayan, & P. R. Montague. (1997). A neural substrate of prediction and reward. *Science, 275*(5306), 1593-1599.

[63] Scott, D. J., E. F. Domino, M. M. Heitzeg, R. A. Koeppe, L. Ni, S. Guthrie, & J. K. Zubieta. (2007). Smoking modulation of mu-opioid and dopamine D2 receptor-mediated neurotransmission in humans. *Neuropsychopharmacology, 32*(2), 450-457.

[64] Seeman, P., H.-C. Guan, & H. Niznik. (1989). Endogenous dopamine lowers the dopamine D_2 receptor density as measured with [^{3}H]raclopride: implications for positron emission tomography of the human brain. *Synapse, 3*, 96-97.

[65] Slifstein, M., & M. Laruelle. (2000). Effects of statistical noise on graphic analysis of PET neuroreceptor studies. *J Nucl Med, 41*(12), 2083-2088.

[66] Srinivasan, R., R. Pantoja, F. J. Moss, E. D. Mackey, C. D. Son, J. Miwa, & H. A. Lester. (2010). Nicotine up-regulates alpha4beta2 nicotinic receptors and ER exit sites via stoichiometry-dependent chaperoning. *J Gen Physiol, 137*(1), 59-79.

[67] Staley, J. K., S. Krishnan-Sarin, K. P. Cosgrove, E. Krantzler, E. Frohlich, E. Perry, J. A. Dubin, K. Estok, E. Brenner, R. M. Baldwin, G. D. Tamagnan, J. P. Seibyl, P. Jatlow, M. R. Picciotto, E. D. London, S. O'Malley, & C. H. van Dyck. (2006). Human tobacco smokers in early abstinence have higher levels of beta2* nicotinic acetylcholine receptors than nonsmokers. *J Neurosci, 26*(34), 8707-8714.

[68] Sullivan, J. M., S. J. Kim, K. P. Cosgrove, & E. D. Morris. (2013). Limitations of SRTM, Logan graphical method, and equilibrium analysis for measuring transient dopamine release with [(11)C]raclopride PET. *Am J Nucl Med Mol Imaging, 3*(3), 247-260.

[69] Takahashi, H., Y. Fujimura, M. Hayashi, H. Takano, M. Kato, Y. Okubo, I. Kanno, H. Ito, & T. Suhara. (2008). Enhanced dopamine release by nicotine in cigarette smokers: a double-blind, randomized, placebo-controlled pilot study. *Int J Neuropsychopharmacol, 11*(3), 413-417.

[70] Urban, N. B., L. S. Kegeles, M. Slifstein, X. Xu, D. Martinez, E. Sakr, F. Castillo, T. Moadel, S. S. O'Malley, J. H. Krystal, & A. Abi-Dargham. (2010). Sex differences in striatal dopamine release in young adults after oral alcohol challenge: a positron emission tomography imaging study with [(1)(1)C]raclopride. *Biol Psychiatry, 68*(8), 689-696.

[71] Volkow, N. D., G. J. Wang, J. S. Fowler, J. Logan, S. J. Gatley, R. Hitzemann, A. D. Chen, S. L. Dewey, & N. Pappas. (1997). Decreased striatal dopaminergic responsiveness in detoxified cocaine-dependent subjects. *Nature, 386*(6627), 830-833.

[72] Volkow, N. D., G. J. Wang, J. S. Fowler, J. Logan, R. Hitzemann, Y. S. Ding, N. Pappas, C. Shea, & K. Piscani. (1996). Decreases in dopamine receptors but not in dopamine transporters in alcoholics. *Alcohol Clin Exp Res, 20*(9), 1594-1598.

[73] Wagner, H. N., Burns, H.D., Dannals, R.F., Wong, D.F., Langstrom, B., Duelfer, T., Frost, J.J., Ravert, H.T., Rosenbloom, J.B., Lukas, S.E., Kramer, A.V., Kuhar, M.J. . (1983). Imaging Dopamine Receptors in the Humans Brain by Positron Tomography. *Science, 221*(4617), 1264-1266.

[74] Weerts, E. M., Y. K. Kim, G. S. Wand, R. F. Dannals, J. S. Lee, J. J. Frost, & M. E. McCaul. (2008). Differences in delta- and mu-opioid receptor blockade measured by

positron emission tomography in naltrexone-treated recently abstinent alcohol-dependent subjects. *Neuropsychopharmacology, 33*(3), 653-665.

[75] Weerts, E. M., G. S. Wand, H. Kuwabara, C. A. Munro, R. F. Dannals, J. Hilton, J. J. Frost, & M. E. McCaul. (2011). Positron emission tomography imaging of mu- and delta-opioid receptor binding in alcohol-dependent and healthy control subjects. *Alcohol Clin Exp Res, 35*(12), 2162-2173.

[76] Yoder, K. K., E. D. Morris, C. C. Constantinescu, T. E. Cheng, M. D. Normandin, S. J. O'Connor, & D. A. Kareken. (2009). When what you see isn't what you get: alcohol cues, alcohol administration, prediction error, and human striatal dopamine. *Alcohol Clin Exp Res, 33*(1), 139-149.

[77] Yoder, K. K., C. Wang, & E. D. Morris. (2004). Change in binding potential as a quantitative index of neurotransmitter release is highly sensitive to relative timing and kinetics of the tracer and the endogenous ligand. *J Nucl Med, 45*(5), 903-911.

[78] Zhou, Y., M. K. Chen, C. J. Endres, W. Ye, J. R. Brasic, M. Alexander, A. H. Crabb, T. R. Guilarte, & D. F. Wong. (2006). An extended simplified reference tissue model for the quantification of dynamic PET with amphetamine challenge. *Neuroimage, 33*(2), 550-563.

IntechOpen